Working Report 2008-62

Sorption of Cesium on Olkiluoto Mica Gneiss and Granodiorite in Saline Groundwater; Retardation of Cesium Transport in Rock Fracture Columns

Jarkko Kyllönen
Martti Hakanen
Antero Lindberg

September 2008

POSIVA OY
Olkiluoto
FI-27160 EURAJOKI, FINLAND
Tel +358-2-8372 31
Fax +358-2-8372 3709

Working Report 2008-62

Sorption of Cesium on Olkiluoto Mica Gneiss and Granodiorite in Saline Groundwater; Retardation of Cesium Transport in Rock Fracture Columns

Jarkko Kyllönen, Martti Hakanen
Laboratory of Radiochemistry
Department of Chemistry
University of Helsinki

Antero Lindberg
Geological Survey of Finland

September 2008

Sorption of Cesium on Olkiluoto Mica Gneiss and Granodiorite in Saline Groundwater; Retardation of Cesium Transport in Rock Fracture Columns

ABSTRACT

Sorption of cesium on Olkiluoto mica gneiss and granodiorite rock types has been studied earlier by batch experiments using crushed rocks and rock slices (Huitti et al., 2000, Huitti et al., 1998). The sorption distribution ratios (R_d) of cesium on the rocks are strongly reduced with increases in salinity and increases in cesium concentration in the solution. In addition, highly nonlinear sorption at elevated cesium concentrations in saline solutions has been found and also very slow desorption of cesium at trace concentrations.

In this work the sorption of cesium on Olkiluoto rocks is studied and a mechanistic cation exchange model is applied for sorption of cesium on Olkiluoto mica gneiss and granodiorite. The sorption of cesium on rock was in accordance with charge balances of cations in a low-salinity groundwater stimulant. Earlier studies have indicated that biotite is the dominating cesium-sorption mineral in fresh mica gneiss, granodiorite and granite. This suggested that a composite additive sorption model for cesium on rocks could be constructed based on the sorption on biotite.

Biotites were separated from the Olkiluoto mica gneiss and granodiorite for biotite specific sorption studies of cesium. The cation exchange capacities of the separated Olkiluoto biotites were almost the same for all the exchangeable cations. The selectivity coefficients of Cs-Na, Cs-K and Cs-Ca cation exchange reactions were determined for the Na-, K- and Ca-conditioned biotites by modelling of the cesium sorption isotherms in the electrolyte solutions. A three-site model is needed to model the sorption over cesium concentration range $1*10^{-8}$ M to $1*10^{-3}$ M isotherms.

Selectivity coefficients determined for the exchange reactions were used in a reactive transport model for migration of cesium in rock fractures at the laboratory scale. The PhreeqC programme was applied. The model was calibrated for migration of cesium in a mica gneiss fracture under constant chemical conditions. The model was applied to modelling of migration of cesium in granodiorite fractures under constant chemical conditions. In this case the sorption site concentrations were reduced owing to the lower biotite content of granodiorite. Modelling of cesium breakthrough during constant concentration inflow in saline groundwater-conditioned mica gneiss and granodiorite was made using the sorption site concentrations for the rock types.

Cesium breakthrough in mica gneiss for $1*10^{-6}$ M Cs in OL-SO was calculated by PhreeqC omitting the sorption on fracture surfaces. The results indicate that in the long run matrix diffusion dominates the breakthrough, but the time of the start of breakthrough is determined by surface sorption. An analytical approach for the same situation with a K_d for sorption and D_e for matrix diffusion was used for comparison. High sorption, a D_e value in accordance with 2% porosity, and omitting the formation factors for the rock porosity were needed to reproduce the long term breakthrough of cesium in an OL-SO-conditioned fracture.

Cesiumin sorptio Olkiluodon kiillegneissiin ja granodioriittiin suolaisessa pohjavedessä; Cesiumin pidättyminen kalliorakokolonneissa

TIIVISTELMÄ

Cesiumin sorptiota Olkiluodon kiillegneissiin ja granodioriittiin on määritetty eräkokein kivimurskeilla ja kivileikkeillä. Massajakautumiskerotoimien arvot pienenevät voimakkaasti veden suolaisuuden tai cesiumpitoisuuden kasvun mukana. Sorption riippuvuus veden cesiumpitoisuudesta on huomattavan epälineaarista ja sorptioon liittyy palautumattomuutta erityisesti suolaisissa vesissä.

Tässä työssä määritettiin cesiumin sorptiota kivileikkeisiin ja laadittiin mekanistinen malli cesiumin sorptiolle Olkiluodon kiillegneissiin ja granodioriittiin. Cesiumin sorption massavaraustasapaino voitiin todeta kokeilla kivileikkeisiin vähäsuolaisessa vedessä. Aikaisemmissa selvityksissä on todettu, että muuttumattomassa kiillegneisissä, granodioriitissa ja graniitissa cesiumin sorptio tapahtuu pääasiassa biotiittiin. Tämän perusteella pääteltiin, että on mahdollista laatia cesiumin sorptiolle mekanistinen malli huomioimalla sorptio pelkästään biotiittiin.

Olkiluodon kiillegneisistä ja granodioriitista erotettiin biotiittia sillä tehtäviä kokeita varten. Biotiiteille määritetyt kationinvaihtokapasiteetit eri vaihtuville kationeille ja cesiumille olivat lähes samat. Na-, K- ja Ca- muotoiseksi muutetuille biotiiteille määritettiin näiden ionien ja cesium kationinvaihdon selektiivisyyskertoimet. Sorptioisotermien tulkintaan tarvitaan malli, jossa biotiitissa on kolme erilaista sorptiopaikkaa, kun liuoksen cesiumpitoisuuden vaihteluväli oli $1*10^{-8}$ M - $1*10^{-3}$ M.

Selektiivisyyskertoimet sijoitettuna PhreeqC malliin tuottivat aiemman eräkokeen kokeellisen sorptioisotermin kanssa hyvin samanlaisen laskennallisen isotermin.

Saatuja selektiivisyyskertoimia käytettiin kiillegneissistä ja granodioriitista laboratoriossa valmistetuille kivirakokolonneille määritetyn cesium kulkeutumisen laskentaan PhreeqC mallilla. Mallin kalibrointiin käytettiin pidättymättömän aineen kulkeutumisen mallinnusta sekä cesiumin kulkeutumista kemiallisesti tasapainoisissa olosuhteissa kiillegneissiraossa. Mallia käytettiin myös cesiumin kulkeutumisen laskentaan kemiallisesti tasapainoisissa olosuhteissa granodioriittiraossa, jossa sorptiopaikkojen määrää pienennettiin kiven pienemmän biotiittipitoisuuden vuoksi. Mallia sovellettiin lisäksi laskentaan, jossa simuloitiin cesiumin läpimurtoa suolaisen OL-SO pohjavesisimulantin kanssa tasapainossa oleville kiillegneissi- ja granodioriittiraolle.

Mallin matriisidiffuusion simulointiin käytetyn osan vaikutusta läpimurtoon verrattiin analyyttiseen aproksimatioon, jossa muuttujina ovat massajakautumiskerroin K_d ja efektiivinen diffuusio matriisiin. Analyyttisessä approksimaatiossa koetuloksia parhaiten kuvaavassa läpimurrossa K_d oli suuri ja D_e arvo matriisin huokoisuutta 2% vastaava kun huokoisuuden muototekijät jätetään huomiotta, kuten myös myös PhreeqC laskuissa. Molemmat laskut osoittivat, että pitkänajan läpitulo oli matriisidiffuusion hallitsema, mutta tässä tehdyissä kokeissa sorptio rakopintaan viivästytti läpimurron alkamista.

TABLE OF CONTENTS

1 INTRODUCTION

Sorption of cesium on Olkiluoto mica gneiss and granodiorite rock types has been studied earlier by batch experiments using crushed rocks and rock slices (Huitti et al., 2000, Huitti et al., 1998, Kaukonen et al., 2000). The sorption distribution ratios (R_d) of Cs on the rocks are strongly reduced with an increase in salinity and Cs concentration of the solution. In addition, high nonlinearity in sorption at elevated Cs-concentrations in saline solutions has been found and also very slow desorption of Cs at trace concentrations. In this work the sorption of Cs on Olkiluoto rocks is studied and a mechanistic cation exchange model is constructed for sorption of Cs on Olkiluoto mica gneiss and granodiorite.

The sorption of cesium on rock slices was studied by determination of sorption mass balances of exchangeable cations in batch experiments by analysis of changes in the concentrations of exchangeable cations in the solutions. The changes are relatively small and the analytical accuracy was sufficient to see the changes only in low-salinity solutions. The results also show that other water mineral interactions than sorption of Cs may effect the solution compositions, especially in long-term experiments and hamper the determination of cation exchange selectivity coefficients for a general composite sorption model.

Earlier studies also indicated that biotite is the Cs sorption dominating mineral in fresh mica gneiss, granodiorite and granite. This suggested that a composite additive sorption model for Cs on rocks could be constructed based on sorption on biotite.

Biotites were separated from the Olkiluoto mica gneiss and granodiorite for biotite specific sorption studies of Cs. The cation exchange capacities of the separated Olkiluoto biotites were almost the same for all the exchangeable cations. The selectivity coefficients of Cs-Na, Cs-K and Cs-Ca cation exchange reactions were determined for the Na-, K- and Ca-conditioned biotites by modelling of the Cs sorption isotherms in the electrolyte solutions. A three-site model was needed to model the sorption for the Cs concentration range $1*10^{-8}$ M to $1*10^{-3}$ M isotherms (Kyllönen et al. 2008).

The selectivity coefficients and the site concentrations of the OLKR9 biotite were used in the PhreeqC programme for modelling of sorption in batch experiments of Cs in the saline groundwater simulate solution on crushed rocks by assuming that the sorption takes place only on biotite. The Cs sorption isotherms for mica gneiss at initial Cs concentrations $6*10^{-8}$ M to $1.1*10^{-3}$ M were successfully modelled (Kyllönen et al. 2008).

The selectivity coefficients were used in a reactive transport model for migration of Cs in rock fractures at the laboratory scale. The PhreeqC programme was applied. The model was calibrated for migration of Cs in a mica gneiss fracture in constant chemical conditions. The model was applied to modelling of migration of Cs in granodiorite fractures at constant chemical conditions and for modelling of breakthrough of Cs during constant concentration inflow in mica gneiss and granodiorite.

2 MATERIALS

2.1 Rock materials

2.1.1 Rock types

The rock samples used in this work were mica gneiss and granodiorite from the Olkiluoto area. Mica gneiss samples were taken from drill core OL-KR9, depth 500-600m. Granodiorite samples were taken from the drill-core OL-KR2, depth 301-391 m. A total of 6.42 m granodiorite and 6.20 m mica gneiss was selected. The rocks were analysed for mineral compositions by point counting of thin sections (Table 1).

Granodiorite
The main minerals in the clearly foliated granodiorite are plagioclase, potassium feldspar, quartz and biotite. Variations in the plagioclase and biotite contents are large within the size of a thin section (20 mm x 30 mm). The mean grain size is 0.3-2.0 mm but the largest feldspar grains are 8-10 mm in diameter. The plagioclase is slightly sericitised. At core length 356 m alteration of biotite to chlorite is considerable. These accessory minerals are common to Olkiluoto granodiorite.

Mica gneiss
The main minerals in mica gneiss are quartz, biotite, plagioclase and feldspar. The mean grain size is 0.5 – 1.0 mm but the sparse cordierite has a grain size up to 8 mm in diameter. The rock is heavily schistose and the composition of the rock varies considerably even in a few centimetres distance. The rock has thin quartz and feldspar rich layers. Aluminium rich minerals cordierite and sillimanite are not homogenously mixed in the rock. Low amounts of opaque minerals (e.g. pyrite) are also found.

Table 2-1. *Compositions (vol-%) of Olkiluoto granodiorite and mica gneiss determined by point counting of thin sections, 500 points/thin section.*

Mineral	Granodiorite 301.50 m	Granodiorite 356.37 m	Mica gneiss 583.85 m	Mica gneiss 597.92 m
Quartz	6.2	23	36.1	32.4
Plagioclase	33.2	44.6	14.5	31.4
K-feldspar	23	17	4.4	0
Biotite	20.2	7.4	27.1	33.6
Sericite	5.2	4	3	0.8
Chlorite	0.6	2.2	0.2	0
Cordierite	0	0	10.9	0.2
Sillimanite	0	0	0.8	1.4
Turmaline	0	0	+	0
Garnet	0	0	+	0
Epidote	0	0.4	0	0
Apatite	+	0.2	0	+
Zirkon	0	+	0.2	+
Opaques	1.6	1.2	2.8	0.2
Total	100	100	100	100

2.1.2 Rock slice samples

Rock slice samples were cut from 42 mm-diameter drilling cores. The planar faces of the slices were grinded even. The slices were quickly rinsed with deionised water and ethanol. The thickness, volume, geometric surface area and weight of a slice were 5 mm, 7 cm^3, 34 cm^2 and 17 g, respectively.

2.1.3 Biotites

Olkiluoto biotites
Pieces of drill cores from boreholes OLKR2 and OLKR9 from depths of 200 - 500 m were crushed to grain size < 0.5 mm. Biotite was separated from rest of the minerals by a magnetic separator and heavy liquid separation. The biotite fractions included some chlorite that was attached to biotite grains. Separation of these two was not possible. The chlorite content of the separated biotite fraction was determined in biotite-epoxy thin sections using the point counting method. The chemical composition of the biotites and chlorite was analysed by a Cameca Camebax SX50- microanalyser. The specific areas of the crushed materials were determined by N_2-BET gas adsorption method (Table 2).

The compositions of KR2 and KR9 biotites were typical of biotites in Olkiluoto (OL) garanodiorite and mica gneiss (Gehör et al. 1996, Lindberg 2002). The chlorite in the separated biotites and the granodiorite and the mica gneiss rock samples is not expected to have a marked impact in the sorption of Cs (Huitti et al. 2003).

Reference biotite
Used as a reference material was a pure pegmatitic biotite (L1) from Luumäki, South-Eastern Finland. This material was earlier used in studies of sorption of Cs on Olkiluoto rock-forming minerals (Huitti et al. 1998).

Table 2-2. *Properties of the biotite samples.*

Sample	KR2	KR9	L1
Particle size	< 0.5 mm	< 0.5 mm	< 0.1 mm
Surface-area (BET)	0.64 m^2/g	0.83 m^2/g	
Biotite	94 %	90 %	
Fe/Mg in biotite	1.82	1.41	
Chlorite	6 %	10 %	

2.2 Waters

2.2.1 Groundwater simulants

Finnish reference groundwater solutions of different salinities were used. The composition of the fresh groundwater simulate (Allard) is typical of shallow granitic bedrock of Finnish inland areas (Vuorinen & Snellman, 1998). The saline groundwater simulant for anaerobic conditions (OL-SR) (Vuorinen et al., 1997) has the composition of the Olkiluoto groundwater at about 500-600 m depth. The OL-SO solution is the carbonate-containing modification of OL-SR. The nominal compositions of the solutions are listed in Table 3. The OL-SO solution was analysed for its main components (Appendix B). The differences from the nominal concentrations were small. Experiments were also made with Allard and OL-SO solutions having higher Cs (CsCl) concentrations.

2.2.2 Electrolyte solutions

0.1 M solutions of NaCl, KCl, CsCl, $CaCl_2$ and $MgCl_2$ were used for determination of exchangeable cations in the biotites. Ammonium acetate solutions and silver thiourea solutions were used for determination of cation exchange capacities of the biotites.

2.2.3 Preparation of solutions

Groundwater simulant solutions and the electrolyte solutions were prepared from (Merck) p.a. and Suprapur quality reagents in ultrapure MILLI-Q-water. The electrolyte solutions were analysed for alkaline and earth-alkaline metals Si and Al by applying ICP-MS, ICP-AES and FAAS methods. The chemical purity of the reagents was satisfactory. The concentrations of impurities were lower than the detection limits of the analysis methods.

Table 2-3. *Compositions of groundwater simulants.*

	OL-SO, pH 7.2		Allard, pH 8.4	
	mg/l	mmol/l	mg/l	mmol/l
HCO^-	10.0	0.16	90.7	1.5
SiO_2	2.5	0.04	2.9	0.05
Na^+	4800	209.1	52.5	2.3
K^+	21.0	0.54	3.9	0.10
Ca^{2+}	4000	100	10.2	0.25
Mg^{2+}	55.9	2.3	2.8	0.11
Sr^{2+}	35.0	0.40		
B^{3+}	0.92	0.08		
SO_4^{2-}	4.2	0.044	9.6	0.10
Cl^-	14500	412.9	47.5	1.3
F^-	1.2	0.063		
Br^-	104.7	1.31		
I^-	0.9	0.007		

2.3 Radioactive tracers

The radioactive tracer isotopes used in the experiments were ^{22}Na, ^{36}Cl, ^{132}Cs, ^{134}Cs and ^{152}Eu. The sort-lived ^{132}Cs isotope was prepared from natural xenon (Xe) gas by bombardment with 10 MeV protons. All other tracers were commercial.

The chemical form was NaCl for ^{22}Na-, ^{36}Cl- and CsCl for ^{134}Cs salt in the stock solutions. These tracers could be used without pH adjustment of the spiked solution. ^{132}Cs was leached directly from the walls of the irradiation target with the OL-SO solution and no pH adjustment was needed. The ^{152}Eu tracer was in 0.1 M HCl solution, and the pH was adjusted before experiments. 4-Morpholine-ethanesulfonic acid (MES) was used in pH adjustment to prevent precipitation of $Eu(OH)_3$ during neutralization of the solution. A 0.1 M NaCl solution was prepared and the MES-concentration was adjusted to 0.06 M. The pH of this solution was 6.8. Acidic ^{152}Eu solution was diluted with this buffer. The pH of the final Eu-152-spiked solution was 6.3. The possible effects of the MES on the sorption of Eu were surveyed by batch experiments. No difference was observed in the sorption of Eu on biotite between the buffered and the non-buffered solution.

3 METHODS

3.1 Water analysis

Allard water
Solutions from rock-water interaction experiments with Allard water were analysed for Na, Ca, Mg, Mn, Fe, Al, Si and Sr with ICP-AES. Cs and K were analysed with ICP-MS.

0.1 M electrolyte solutions
The exchangeable cations in the electrolyte solutions in the cation exchange capacity determinations and in biotite conditioning effluents were measured with flame atomic absorption spectrophotometry (FAAS).

OL-SO solution
The composition of the OL-SO solution was analysed for its main cations. The elements Ca, Mg, Na and Sr were determined by ICP-AES and K, and Cs by ICP-MS.
The STD of 14 replicate determinations were 0.7%, 1.5%, 0.9%, 0.7% and 3.4% for Ca, Mg, Na, Sr and K, respectively. For the Cs 0.5 μg/L ($3.7x10^{-7}$ mol/L) concentration the STD was 28%. This indicates that the accuracy of the determinations of the major components is not good enough to see changes in OL-SO composition induced by the solution-mineral interactions.

Cs determinations for OL-SO solutions with no added Cs tentatively showed an increase of 3-9 μg/L in Cs concentration after interaction with granodiorite rock slices. This was equivalent to a Cs concentration of $2\text{-}7*10^{-8}$ M.

Measurement of pH
The pH of the solutions was measured with Radiometer combination glass/AgCl electrodes. The measurement systems were calibrated using commercial pH standard buffer solutions.

3.2 Radioactivity counting of liquid samples

The radioactivity assay of ^{36}Cl in solution samples was done by liquid scintillation counting (Wallac Rackbeta 1219). The gamma emitting isotopes ^{22}Na, ^{132}Cs, ^{134}Cs and ^{152}Eu in solution samples were counted using gamma spectrometers (Wallac 1280 Ultrogamma or Wallac Wizard 1480 3” gamma spectrometers).

3.3 Radioactivity counting of rock samples

The distributions of Cs (^{134}Cs) along the flow path on fracture surfaces for two dismantled columns were scanned with a single channel gamma-activity Na(Tl)I detector using a 10 mm slit collimator.

3.4 Sorption of cesium on rocks

3.4.1 Mass balance in sorption to the rock types

The mass balance in sorption of cesium to rocks was surveyed by analysis of the changes in exchangeable cations and silicon concentrations in the Cs-added Allard waters after contact with rock slices. Granodiorite and mica gneiss slices were put into 100 ml polyethylene vessels, four slices (140 cm^2, 68 g) in each vessel. The slices were in a vertical position on a PVC-disc which had slots for the slices. The rocks were fresh, either non-conditioned or conditioned with Allard solution.

The vessels were filled with 70 ml of Allard water with Cs concentrations $1*10^{-8}$ M to $1*10^{-3}$ M. Parallel samples with ^{134}Cs-spiked solutions were prepared for the determination of sorption of Cs. Allard water-filled vessels without rock were included as background samples. The cation concentrations in the solutions were analysed after a contact time of one week, two months and one year.

3.4.2 Long term sorption on the rock types

Differences in sorption capacity of the rock types for Cs were surveyed in experiments where the water was substituted several times with a new solution. Allard and OL-SO solutions with ^{134}Cs-spiked Cs at concentrations $5*10^{-6}$ M and $5*10^{-4}$ M were used. The aliquots taken for ^{134}Cs measurement were filtered through a 0.22 µm membrane filter. The solutions were changed 7 times. The total amounts of Cs that were sorbed on the rocks were derived from the ^{134}Cs activity measurements.

3.4.3 Sorption isotherms of cesium for rocks

Sorption of Cs on granodiorite and mica gneiss slices was studied as a function of Cs-concentration. The slices were preconditioned with OL-SO solution before the water was changed to (^{134}Cs-spiked) Cs-added OL-SO. The Cs-concentrations were $1*10^{-8}$ to $1*10^{-3}$ M. The exposure times were 3 days, 3 weeks and 7 weeks. ^{134}Cs activity in solution was measured to determine the sorption of Cs. The aliquots for the ^{134}Cs measurements were filtered through a 0.22 µm membrane.

3.5 Sorption of cesium on biotites

3.5.1 Cation exchange capacities (CEC) of the biotites

Sorption capacity for alkaline and earth-alkaline cations
The cation exchange capacity of biotites for Cs^+, Na^+, K^+, Mg^{2+} and Ca^{2+} was surveyed by batch experiments. Polyethylene vessels were used. 0.8 g of biotite was mixed with 8 ml of 0.1 M solution of CsCl, NaCl, KCl, $CaCl_2$ or $MgCl_2$. After a contact time of one day the solution was separated by centrifugation, acidified with Suprapur HNO_3 and analysed for the exchangeable cations.

Sorption capacity for silver cation
The silver-thiourea (AgTU) method (Chhabra et al. 1975) was applied. 1 g biotite was weighed into a 50 ml centrifuge tube, and 30 ml solution was added. The tubes were shaken overnight, centrifuged and the solution was filtered with a 0.22 μm membrane. The solution samples were acidified with Suprapur HNO_3 and analysed for the exchangeable cations.

Sorption capacity for ammonium ion
The ammonium acetate method was applied by determining the exchangeable cations in solution. 1 g of biotite was mixed with 10 ml of 1 M NH_4Ac solution. The solutions were separated from the biotites after contact times from one day to 152 days. The solutions were acidified with Suprapur HNO_a and analysed for alkali and alkaline earth cations.

3.5.2 Selectivity coefficients of exchange of Cs^+ for bound Na^+, K^+ and Ca^{2+}

Conditioning of biotite
KR9 biotite was conditioned to Na-, K- and Ca-forms by 0.1 M solutions of KCl, NaCl and $CaCl_2$ for determination of cation exchange selectivity coefficients. A column setup was used to keep the leaching solution as pure as possible. The effluents were analysed by ICP-MS for the exchangeable cations. Conditioning was continued until concentrations of the other exchangeable cations were lower than 1% of their concentrations in the first effluent fractions.

Determination of the cation occupancies
Cs sorption experiments were performed with the Na-, K- and Ca-conditioned biotites. 0.1 M solutions of NaCl, KCl and $CaCl_2$ containing $1*10^{-8}$ -$1*10^{-4}$ M of Cs (spiked with ^{134}Cs) were equilibrated with the Na-, K- and Ca-form of biotite, respectively. Sorption of Cs was determined at pH 6 and pH 8 and the cation occupancies were calculated for derivation of selectivity coefficients.

3.6 Fracture migration experiments

3.6.1 Fracture columns

Fracture columns were constructed of granodiorite and mica gneiss. 25 cm-long, 42 mm-diameter drill core pieces were cut to four quadrants along the core axis. The planar faces (2 cm x 25 cm) of these were ground flat and rinsed with deionised water and ethanol. The flat surfaces of two 12 - 13 cm-long core quadrants formed the fracture walls. The fracture aperture was adjusted to 0.2 mm using plastic film between the edges of flat surfaces. The fracture flow channel width was adjusted to 5 mm. PEEK tubing with an internal diameter of 0.50 mm was attached to the fracture ends. The length between the fracture inlet and outlet was about 110 mm. The outer parts of columns were covered with a layer of polyurethane (Sikaflex) and the columns were further covered with polystyrene (Plastic Padding) to have sufficient mechanical strength. A list of the columns is given in Table 3.

Table 3-1. *Dimensions of the columns.*

Column	Rock type	Nominal dimensions outer length*fracture width*aperture
G1	granodiorite	13 cm*5 mm*0.2 mm
G2	granodiorite	13 cm*5 mm*0.2 mm
GD1	granodiorite	13 cm*5 mm*0.2 mm
GD2	granodiorite	13 cm*5 mm*0.2 mm
GD3	granodiorite	12.5 cm*5 mm*0.2 mm
GD4	granodiorite	12.3 cm*5 mm*0.2mm
K1	mica gneiss	13 cm*5 mm*0.2 mm
K2	mica gneiss	13 cm*5 mm*0.2 mm
KG1	mica gneiss	13 cm*5 mm*0.2 mm
KG2	mica gneiss	13 cm*5 mm*0.2 mm
KG3	mica gneiss	12.6 cm*5 mm*0.2 mm
KG4	mica gneiss	12.7 cm*5 mm*0.2 mm

3.6.2 Flow rates

Peristaltic pumps (ISMATEC IPN) with adjustable flow rates were used. Flow rates of 0.9 to 2.5 µl/min were achieved by using 0.2 mm internal diameter Tygon tubes. The volumetric flow rates were determined by weighing of effluents.

3.6.3 Injection of tracer

Continuous injection was maintained by immersing the pump tube end in the ^{134}Cs-spiked solution. Pulse injections of Cs and Eu tracers were made using Rheodyne injectors that were attached to the column inlet tube. The loop was a 5 µl PEEK tube loop (Rheodyne 9725) or a 1 µl internal loop (Rheodyne 7410).

3.6.4 Collection of effluent

The effluent was collected with a programmable fraction collector (Pharmacia-LKB, Readyfrac). The smallest effluent fraction volume was minimised by inserting a flusher unit to the column outlet tube end (Figure 3-1). This enabled time-based fraction collection of small effluent volumes.

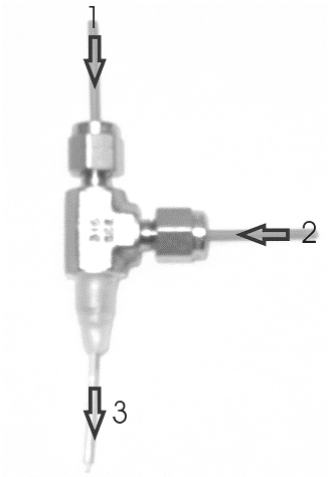

Figure 3-1. *Flusher unit. Tubing from the column outlet is attached to inlet "1" and goes through the unit to outlet "3". The flushing solution tubing inlet is attached to "2"and the outlet to"3" to flush the effluent tubing tip.*

3.6.5 Conditioning of rock surfaces

All migration experiments were performed in saline solution conditions. The OL-SO solution was pumped through the columns to condition the rock surfaces. The conditioning period before the tracer experiments was more than three months. The flow rate was 2.5 µl/min, and the minimum flow-through volume during this period was equal to or larger than 2500 column volumes.

3.6.6 Conditioning of rock surfaces

The flow properties of the columns were surveyed by determination of breakthrough time distribution of a pulse injected non-sorbing ^{36}Cl tracer. These experiments were made also for the PEEK tubing of appropriate length. The ^{36}Cl experiments were done for all columns at the end of the conditioning period using a flow rate of 2.5 µl/min. ^{36}Cl- breakthrough was also measured at the flow rate of 1 µl/min for the columns used in the pulse-injection experiments of Cs.

3.6.7 Breakthrough of Cs in the OL-SO conditioned columns

After conditioning of the columns the OL-SO solution was changed to ^{134}Cs-spiked Cs-OL-SO that was continuously introduced to mica gneiss and granodiorite columns. The inflow Cs concentrations were 10^{-7} M, 10^{-6} M and 10^{-4} M. The effluents were collected and the ^{134}Cs activity was measured. The breakthrough time distributions were derived.

3.6.8 Migration of Cesium in Cs-OL-SO conditioned fractures

The aim was to study migration of Cs in constant chemical conditions in a rock fracture that is in equilibrium with both OL-SO and a known Cs concentration. A steady state of chemical conditions was assumed when the ^{134}Cs activity concentration in the inflow

and the effluent were the same. The migration of Cs was determined by recording the breakthrough time distribution of ^{132}Cs after a 1 µl injection of ^{132}Cs-spiked Cs-OL-SO. The ^{132}Cs experiments were performed using a flow rate of 1.0 ± 0.1 µl/min.

3.6.9 Migration of europium in OL-SO conditioned fractures

Two experiments were made with ^{152}Eu to study the possible effects of absorption of Cs on the mineral surfaces on the migration of Eu. Experiments were done with a column that was equilibrated with Cs-OL-SO with a Cs concentration of 10^{-6} M and with a OL-SO conditioned column. The flow rate was 1.1 µl/min.

4 EXPERIMENTAL RESULTS

4.1 Mass balance in sorption to rocks

4.1.1 Sorption to non-conditioned rocks

The mass balance was surveyed by changes in compositions of the waters. Changes in Cs, Na, Mg, Al, Si, K, Ca and Sr concentrations in the Allard water samples are presented in Figures A-1 to A-8 in Appendix A.

The sorption of cesium is regarded as a cation exchange reaction and takes place preferentially on dark minerals, especially on biotite. In the reaction Cs is exchanged for a cation on the mineral. The results indicate that mineral-solution interactions other than sorption of Cs influence more strongly the cation composition of the solution.

A rapid decrease in Cs concentration is observed (Figure A1). Sorption of Cs on garanodiorite continues through the whole experimental period in samples with an initial Cs concentration of $5*10^{-4}$ mol/l. After one year the sorbed amount is about two times that after one week. The final decrease in solution concentration is 0.173 mol/l. Sorption of Cs on mica gneiss continues rapidly also after the first week. The decrease in Cs solution concentration is 0.50 meq/l after nine weeks and 0.48 meq/l after one year indicating no increase in the long run.

The figures A1-A8 (Appendix A) indicate that there were both increases and decreases in the solution concentrations of the various cations. Sodium concentrations increased in all solutions, increasing in mica gneiss more than in garanodiorite samples. At the same time the Ca concentrations in mica gneiss samples decreased but in garanodiorite samples there was an increase in the solution concentrations. The behaviour of the other earth-alkaline cations Mg and Sr was very much the same as that of Ca. The K concentrations decreased but in the $5*10^{-4}$ mol/l Cs sample the decrease was smaller than in the lower Cs concentration solutions. The K concentration changes were more like that of the alkaline earths than that of Na.

The time behaviour of the concentration changes of Na, K, Mg, Ca and Sr was for the different rock types about the same as in sorption of Cs. The sample water anion analysis after one year's experiment showed that there was also increases in especially chloride, fluoride and sulphate concentrations. The Al and Si concentrations in the solutions (Figures A-4 and A-5) indicate that there was also some dissolution of the minerals. The increase in anion concentrations and increase in (dissolved) silica compensate for the calculated net positive charge increases by the cations in the solutions. The sum of the one year values for the exchangeable cations is lower in mica gneiss and higher in granodiorite sample solutions than in the Allard solution.

The Si concentrations in figure A-5 for the Allard solutions indicate that there was some dissolution of the rocks. The changes are small but the order of change is from smallest to highest Cs concentration for both rock types. The Al concentrations vary only a little. There are some indications that sorption of cations increase the dissolution of silica and feldspar, with cesium inducing higher increases than the other alkaline cations (Dove

1995). The results suggest that Cs in solution has an enhancing effect on mineral dissolution even at low concentrations but the effect is not directly proportional to sorption of Cs. As compared to increases in cation concentrations, both the Al and Si concentrations vary little. This may indicate re-adsorption of these on the mineral surfaces or formation of silica precipitates as reviewed by Dove (1995) and Blum and Stillings (1995).

4.1.2 Sorption to Allard water conditioned rocks

The effect of sorption of Cs at $1*10^{-8}$ mol/l and $5*10^{-6}$ mol/l on the mmol/l level concentrations of the main cations should be negligible and the mean of these analysed values were used as background concentrations when the changes in the cation compositions owing to sorption of Cs from the initially $5*10^{-4}$ mol/l Cs were calculated (Table 4-1 and 4-2). The differences between the cation concentrations should be due to exchange for Cs. The 1 week values for both the mica gneiss and granodiorite samples for the decrease in Cs charge equivalent concentration and the increase in sum of the main cation charge equivalents are in total agreement. For the mica gneiss the net equivalent changes for the two months and one year samples are in fair agreement. For the granodiorite sample solutions only the values for one week of Cs sorption are in fair exchange balance. For the longer contact times there is additional increase in Na and Ca concentrations, probably due to dissolution of plagioclase.

The one week Cs sorption samples indicate that very little potassium is released even when it is known that Cs is sorbed mainly on biotite and the exchangeable cation in pure biotite is expected to be the potassium cation. Obviously the sorption of Cs on the mica gneiss and granodiorite rocks is not mainly by exchange of K for Cs in biotite.

Table 4-1*. Changes in Allard water cation compositions owing to sorption of cesium on OL mica gneiss at $5*10^{-4}$ mol/l (0.5 meq/l) initial Cs concentration.*

Element	meq/l, 1 week *	meq/l, 2 months *	meq/l, 1 year *
Cs	-0.30	-0.49	-0.48
K	0.10	0.04	0.02
Ca	0.29	0.07	0.17
Mg	0.09	0.01	0.04
Na	-0.20	0.48	0.374
sum K,Ca,Mg,Na	0.28	0.60	0.60

* Differences between element concentrations in initially $5*10^{-4}$ mol/l and $5*10^{-6}$ mol/l Cs concentration solutions.

Table 4-2. *Changes in Allard water cation compositions owing to sorption of cesium on OL granodiorite at $5*10^{-4}$ mol/l (0,5 meq/l)initial Cs concentration.*

Element	meq/l, 1 week *	meq/l, 2 months *	meq/l,1 year *
Cs	-0.08	-0.11	-0.17
K	0.00	0.05	0.06
Ca	0.04	0.13	0.10
Mg	0.01	0.03	0.05
Na	0.03	0.02	0.39
sum K,Ca,Mg,Na	0.08	0.23	0.50

* Differences between element concentrations in initially $5*10^{-4}$ mol/l and $5*10^{-6}$ mol/l Cs concentration solutions.

4.2 Long-term sorption of cesium on rock slices

The Cs-OL-SO waters of the sample vessels were changed seven times. The ^{134}Cs-spiked solutions were changed to a new solution of the same original Cs concentration four times at one weeks interval, and then after two weeks. The amounts that were sorbed on the rocks at times of solution change are indicated in figure 4.16 for granodiorite and in figure 4.17 for mica gneiss.

Sorption at the $5*10^{-6}$ M Cs concentration was highest for both rock types from the first water. In mica gneiss there was a slight continuous decrease in sorption from the renewed solution from week 1 to week 6. For the longer exposure times the sorption on mica gneiss was the same for the period of days 42 to 186 and from day 186 to day 560 indicating very mild time dependence. In the granodiorite the longer exposure time was followed by higher sorption. At the higher $5*10^{-4}$ M Cs concentration the sorption of Cs on mica gneiss followed the same trend as at the lower $5*10^{-6}$ mol/l Cs concentration. There too, the sorption was the same between days 42 to 186 and 186 to 560. The sorption on the granodiorite after the slightly higher sorption at week two than at week one was followed by nearly the same sorption for the following waters during weeks 3 to 6. Between days 42 and 186 and 186 and 560 the sorption was the same but slightly lower than during the first weeks. Here too the time dependence in sorption was weak for the long exposure times.

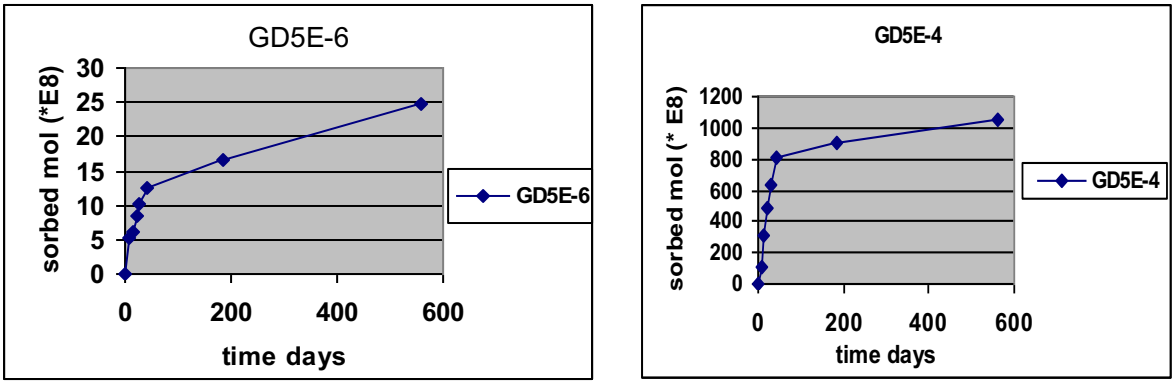

Figure 4-1. *Sorption of Cs in moles to granodiorite slices from OL-SO solutions for Cs concentrations $5*10^{-6}$ M and $5*10^{-4}$ M.*

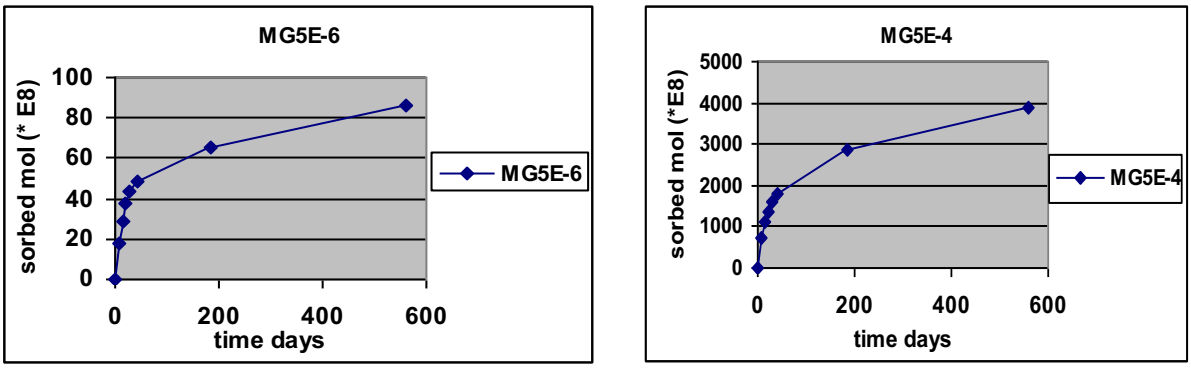

Figure 4-2. *Sorption of Cs in moles to mica gneiss slices from OL-SO solutions for Cs concentrations $5*10^{-6}$ M and $5*10^{-4}$ M.*

For the two Cs concentrations used the amounts of sorbed Cs at day 560 in the mica gneiss were 6.1 neq/cm^2 and 270 neq/cm^2 and in the granodiorite 1.8 neq/cm^2 and 75 neq/cm^2 for the geometric surface area. For both Cs solutions mica gneiss adsorbed about 3 times more Cs than granodiorite. The difference in the sorbed amounts of Cs to the rock types were in accordance with the amount of biotite in the rock types. At these Cs concentrations no saturation in sorption was found. The highest amount of Cs sorbed in the mica gneiss was 10% and in the granodiorite 7% of the CEC of biotite in the rock types (Chapter 4.4).

4.3 Sorption isotherm of cesium for mica gneiss and granodiorite

The sorption isotherms of Cs for mica gneiss and granodiorite slices in OL-SO solution are given in Figure 4.3. In these experiments the sorption on mica gneiss exhibits the very non-linear sorption behaviour at higher than natural Cs concentrations. This has been previously seen for Hästholmen (Huitti et al. 2000) granite and biotite and

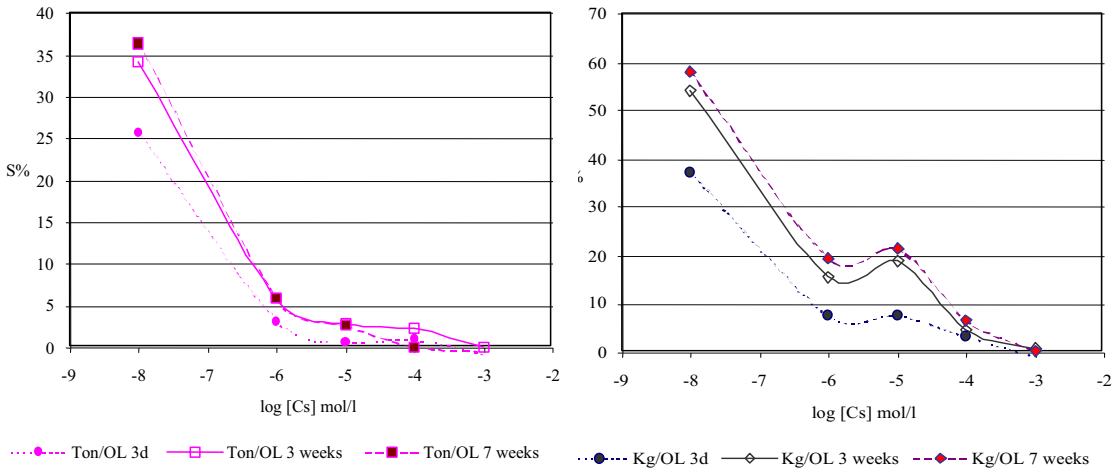

Figure 4-3. *The sorption of Cs (sorption %) to Olkiluoto granodiorite (Ton) and mica gneiss (Kg) as a function of the initial Cs concentration in OL-SO solution.*

Olkiluoto rocks and biotites. In this experiment the sorption at initial Cs concentration $1*10^{-5}$ M is about two times higher than if there was no non-linearity. The strong sorption non-linearity connected to possible irreversibility has been typical to sorption in Na- and Ca-rich brackish and saline solutions. The mechanism behind this could not be seen in the mass balance surveys for the rock types. Strong non-linearity and irreversibility of Cs sorption to altered biotite in a very saline solution has been traced to take place between biotite lamellae in Hanford sediments (Zachara et al. 2000).

4.4 Sorption of cesium on biotite

4.4.1 Cation exchange capacity of KR2 and KR9 biotites

Cation exchange capacities were determined using the Ag-TU-standard method (Chhabra et al. 1975), ammonium acetate method (Chapman et al. 1965) and 0.1 M solutions of NaCl, KCl, CsCl, $CaCl_2$ and $MgCl_2$. CEC was calculated as the sum of the released cations as charge equivalents (Tables 4-3 and 4-4). Median values of CEC for the KR2 and KR9 biotites were derived. The CEC values for the NH_4Ac method were the lowest, the main difference being in smaller K release. Increases of K and Mg concentrations with time for the NH_4Ac solution suggest that these values are affected by dissolution of the biotites more than slow exchange kinetics in the long run in these experiments (Table 4-5). The impacts of Na and Ca concentrations released from KR2 and KR9 are high as compared to the reference biotite L1 in which K^+ and Mg^{2+} are the dominating exchangeable cations in the extraction solution in accordance to other pegmatitic biotites studied in our laboratory. The CEC values for the different biotites indicate that the magnitude of the CEC increased with decrease in grain size (APPENDIX B). The CEC value selected to be used in sorption modeling of the OL biotites is 0.018 meq/g.

Table 4-3. *CEC of OL KR9 biotite.*

Solution	K µeq/g	Na µeq/g	Mg µeq/g	Ca µeq/g	CEC µeq/g
0.1 M NaCl	4.3	2.1*	0.7	7.7	14.8
0.1 M CsCl	5.2	2.0	0.8	9.2	17.2
0.1 M KCl	6.7*	2.1	1.2	5.9	15.9
0.1 M $CaCl_2$	6.7	2.2	1.3	7.4*	17.6
0.1 M $MgCl_2$	7.8	2.0	1.25*	5.1	17.5
AgTU	10.6	2.7	1.4	7.4	22.1
Median	6.7	2.0	1.25	7.4	17.6
1 M NH4Ac, 1 d	1.2	1.6	1.4	7.3	11.5
1 M NH4Ac, 5 d	1.8	1.2	2.8	7.6	13.9

* median value released by the other electrolyte solutions

Table 4-4. *CEC of OL KR2 biotite.*

Solution	K µeq/g	Na µeq/g	Mg µeq/g	Ca µeq/g	CEC µeq/g
0.1 M NaCl	6.1	1.7*	0.5	5.2	13.5
0.1 M CsCl	4.5	1.7	0.8	7.2	14.2
0.1 M KCl	7.8*	1.8	1.7	7.4	18.7
0.1 M $CaCl_2$	8.0	1.8	1.2	7.3*	18.3
0.1 M $MgCl_2$	10.2	1.6	1.2*	5.5	18.5
AgTU	7.8	3.9	1.2	8.1	21.0
median	7.8	1.7	1.2	7.3	18.3
1 M NH4Ac, 1 d	1.2	1.3	1.15	7.7	11.4
1 M NH4Ac, 5 d	1.8	1.3	2.5	9.2	14.8

* median value of this cation released by the other electrolyte solutions

Table 4-5. *Exchangeable cations (µeq/g) released from OLKR2, OLKR9 biotites and pegmatitic biotite L1(< 0.1mm grain size) in 1 M NH_4Ac solution.*

biotite	time d	Mg µeq/g	K µeq/g	Ca µeq/g	Na µeq/g	CEC µeq/g
KR2	1	1.31	1.21	7.85	1.31	11.4
KR2	1	1.11	1.18	7.61	1.27	11.2
KR2	6	2.52	1.76	9.14	1.26	14.7
KR2	6	2.50	1.73	9.28	1.33	14.9
KR2	13	4.33	2.33	10.0	1.30	18.0
KR2	152	27.6	11.4	17.0	1.75	57.8
KR9	1	1.36	1.23	7.23	1.56	14.5
KR9	1	1.41	1.20	7.33	1.63	11.6
KR9	6	2.74	1.84	7.51	1.68	13.8
KR9	6	2.87	1.83	7.69	1.68	14.1
KR9	13	4.67	2.39	7.44	1.66	15.9
KR9	152	29.3	11.9	12.1	2.29	55.6
L1	1	36.0	54.0	1.53	1.25	92.9
L1	1	36.5	49.2	1.54	1.14	88.4
L1	6	40.0	55.9	1.56	1.34	98.8
L1	13	48.8	59.4	1.57	1.38	111.2

4.4.2 Cesium sorption isotherms for conditioned biotites

The sorption isotherms of Cs in 0.1 M NaCl, KCl and $CaCl_2$ solutions at pH 6 and at pH 8 are plotted in Figure 4-4.

It is to be noted that for the Na- and Ca-conditioned biotite the sorption of Cs at pH 6 increases strongly at Cs loading higher than 0.2 ueq/g (1% of CEC) at Cs equilibrium concentration of $1*10^{-5}$ M (Figures 4-4 and 4-5). Otherwise there is practically no pH dependency in Cs sorption on the biotites. It is noted that the start of the increase in sorption of Cs with increase in cesium concentration coincides with that for strong non-linearity in Cs sorption isotherm on the mica gneiss in OL-SO solution.

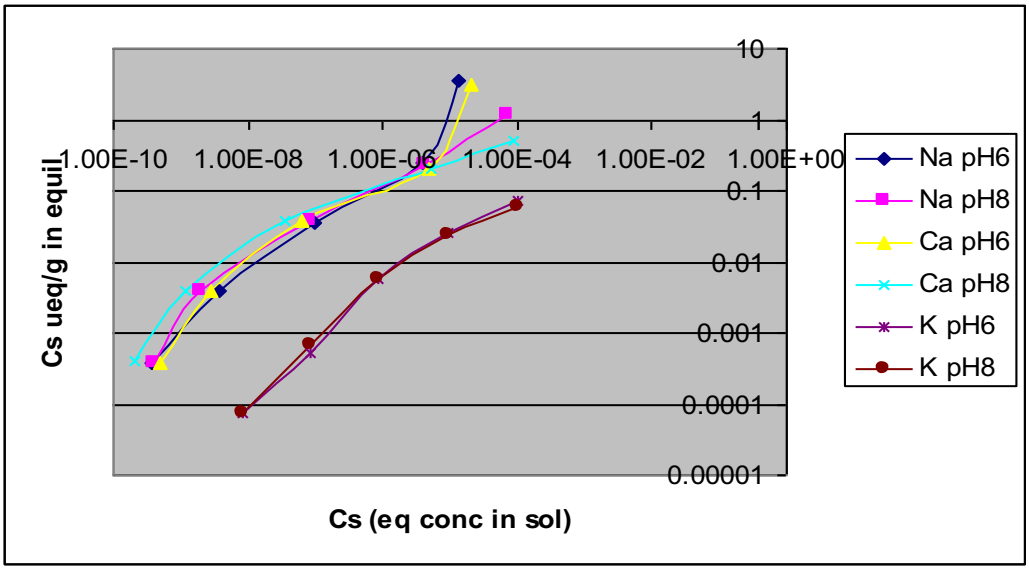

Figure 4-4. *Sorption isotherms of Cs for Na-, K-, and Ca- conditioned KR9 biotite in resp. 0.1 M NaCl, KCl and $CaCl_2$ at pH 6 and at pH 8.*

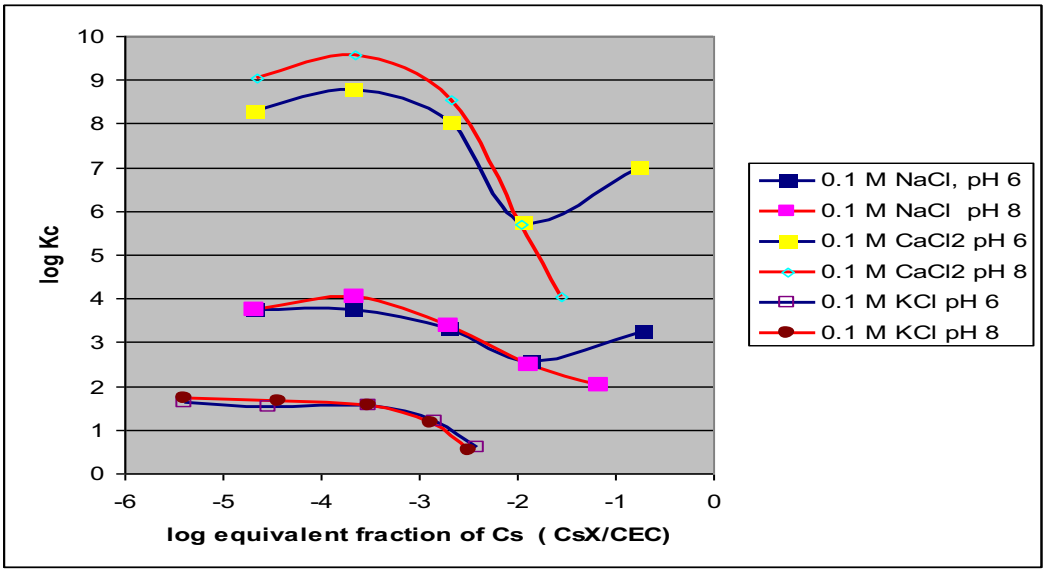

Figure 4-5. *Conditional reaction equilibrium constants (Kc) for Cs sorption on Na-, K-, and Ca-conditioned KR9 biotite.*

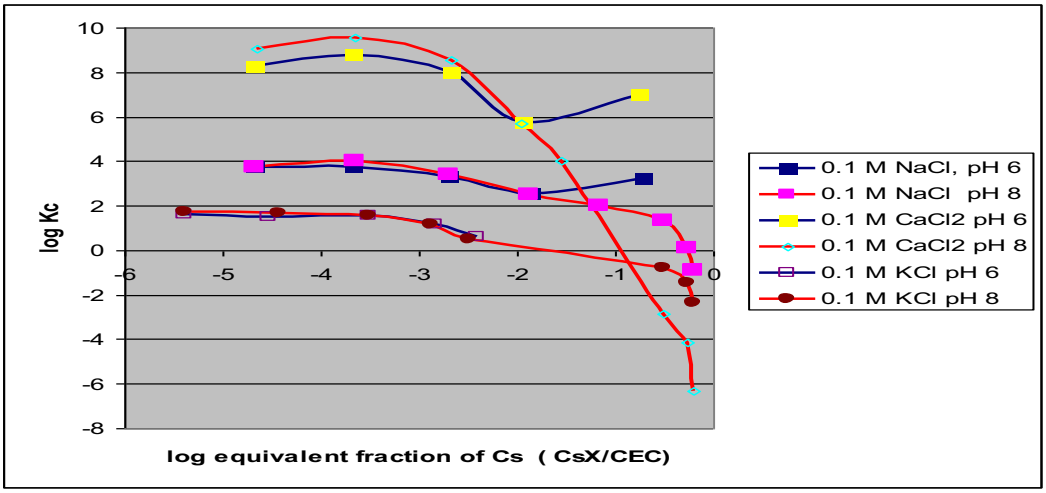

Figure 4-6. *Dependence of conditional G/T selectivity coefficient of Cs exchange for Na, K and Ca in conditioned OL-KR9 biotite and unconditioned OL-KR2 biotite (see text).*

Conditional selectivity coefficients (Figure 4.5) using the Gaines and Thomas convention were derived from the site occupancies assuming that there was only one type of sorption site.

The conditional selectivity coefficients for Cs concentrations $1*10^{-4}$ M to $1*10^{-1}$ M were derived from the experiments of sorption of Cs on the unconditioned KR2 biotite (Figure 4-6). In these conditions K, Na and Ca were minor solution components. At high Cs site occupancy the selectivity of Cs against K, Na and Ca is low. The mechanistic modeling of the isotherms is presented in Kyllönen et al (2007). The high

solution Cs concentrations are not expected in bedrock conditions and the modeling was limited to Cs equilibrium concentration lower than or equal to $1*10^{-4}$ M. The Gaines & Thomas selectivity coefficients for the exchange and the site densities for the three sorption sites are given in Table 4-6.

Table 4-6. *Equlibrium constants for exchange of Cs, K and Ca for bound Na in OL biotite. The proportions of the different sorption sites are also given. (Kyllönen et al. 2008)*

Reaction	logK
Cs+ + NaX = CsX + Na+	2
Cs+ + NaXa = CsXa + Na+	4.5
Cs+ + NaXb = CsXb + Na+	8
K+ + Na X = KX + Na+	2.3
K+ + NaXa = KXa + Na+	2.3
K+ + NaXb = KXb + Na+	2.5
Ca^{2+} + 2NaX = CaX_2 + $2Na^{+}$	0.6
Site	% of CEC
X	95
Xa	4.98
Xb	0.02

4.5 Migration of cesium in rock fractures

4.5.1 Column flow properties

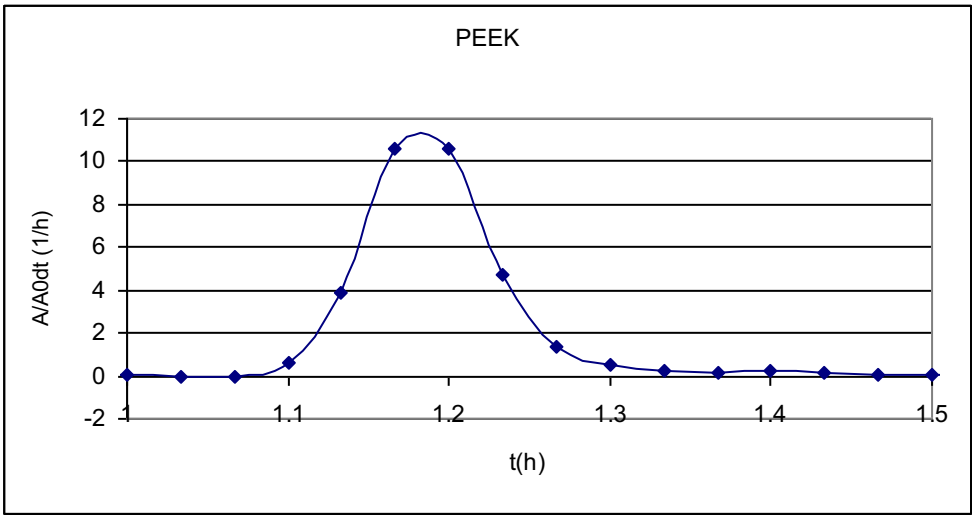

Figure 4-7. *^{36}Cl breakthrough from the PEEK tubing used in columns KG1-KG and GD1-GD4. A0 is the injected activity, flow rate 2.5 µl/min. Volume of the tubing is 170 ul.*

Flow properties of the columns were determined twice: before the start of OL-SO conditioning and just before Cs injection. Breakthrough time distributions of the non-sorbing tracer (^{36}Cl peaks) were symmetrical and a maximum of ^{36}Cl concentration when only the PEEK tubing was surveyed coincided with the tubing volume. The maximum in ^{36}Cl break through activity concentration was at 85-115 µl for the rock columns when corrected for the tubing volume. This is in fair agreement with the target volume (100 ul) of the columns (Figures 4-8, 4-9).

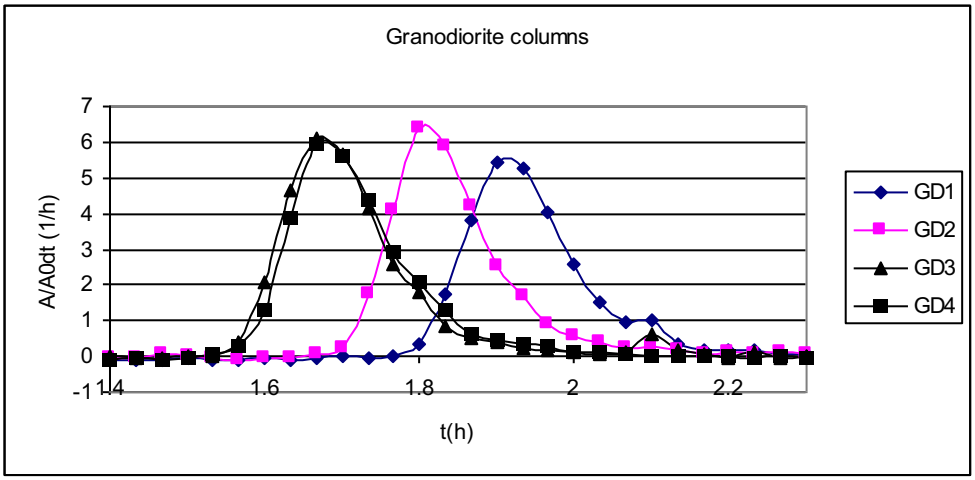

Figure 4-8. *^{36}Cl breakthrough from the granodiorite columns GD1-GD4. A0 is the injected activity, flow rate 2.5 µl/min.*

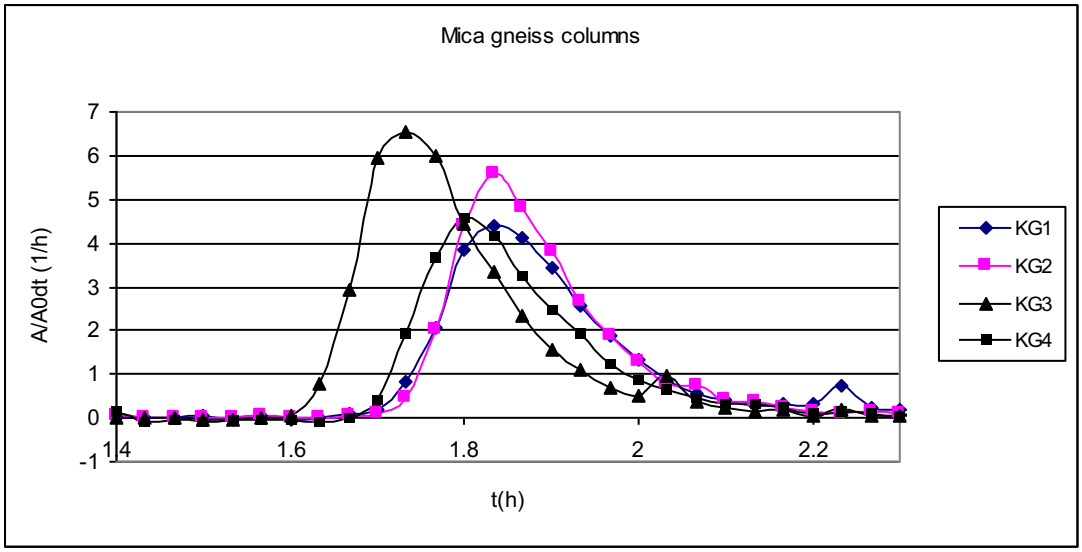

Figure 4-9. *^{36}Cl breakthrough from the mica gneiss columns KG1-KG4. A0 is the injected activity, flow rate 2.5 µl/min.*

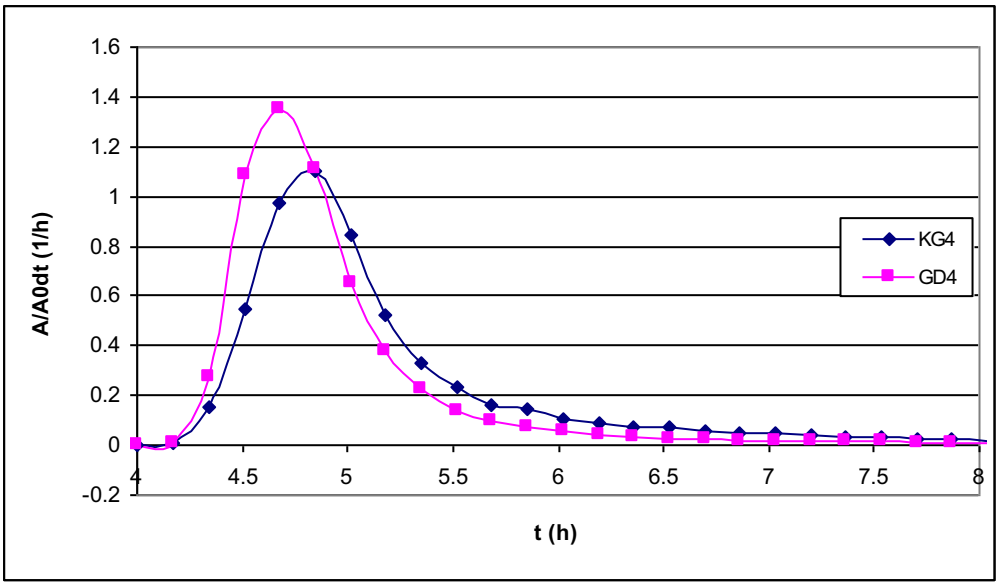

Figure 4-10. *^{36}Cl breakthrough on columns KG4 and GD4, flow rate 0.9 µl/min.*

Table 4-7. *Peek tubing and column volumes*

Identifier	Volume (µl)
Peek /K,G columns	90
Peek / KG,GD columns	170
KG1	105
KG2	105
KG3	90
KG4	100
GD1	115
GD2	100
GD3	85
GD4	85

4.5.2 Breakthrough of cesium in OL-SO-conditioned fracture columns

The OL-SO solutions were spiked with ^{134}Cs-labeled Cs to concentrations $1*10^{-7}$ M, $1*10^{-6}$ M and $1*10^{-4}$ M. The breakthrough was measured after start of Cs-OL-SO introduction with a flow rate 0.9 µl/min for mica gneiss at $1*10^{-7}$ M Cs. All other columns were surveyed with a flow rate 2.5 µl/min.

Figure 4-11 indicates breakthrough at $1*10^{-6}$ M Cs in mica gneiss and in granodiorite. The breakthrough curves for the rock types indicate higher sorption capacity of mica gneiss. This is in accordance with the earlier batch sorption experiment with these rock types.

Breakthrough of Cs at $1*10^{-7}$ M in mica gneiss (Figure 4-12) shows very close similarity with that in mica gneiss at 10 time higher Cs concentration. The slope of increase in Cs concentration is even lower.

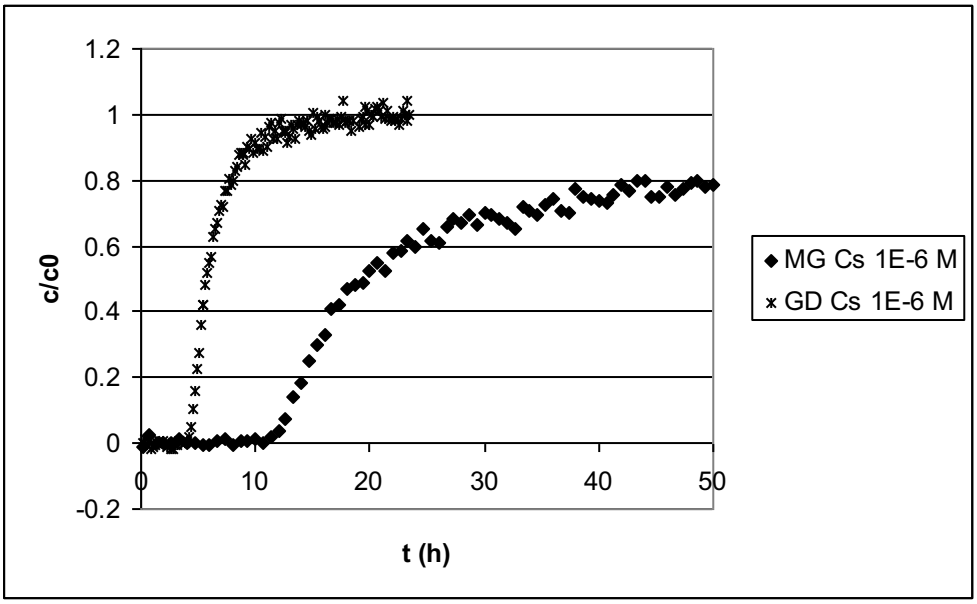

Figure 4-11. *Cs breakthroughs after start of continuous Cs feeding in mica gneiss (MG) and granodiotite (GD), Cs concentration $1*10^{-6}$ M. C_0 is the Cs concentration in the inflowing solution. Flow rate 2.5 µl/min. Time 0 is the time of injection.*

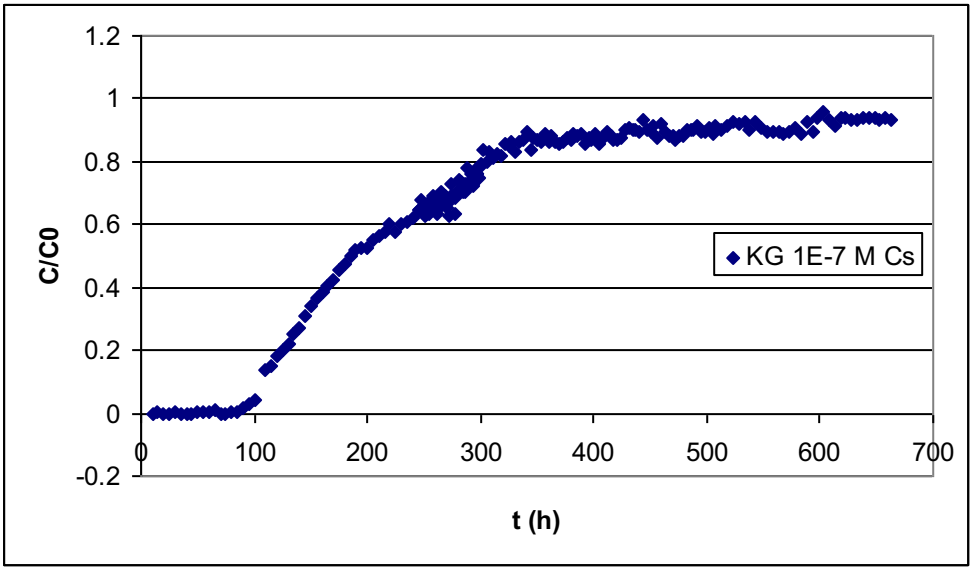

Figure 4-12. *Cs breakthrough after start of continuous Cs feeding in mica gneiss (KG), Cs concentration $1*10^{-7}$ M. C_0 is the Cs concentration in the inflowing solution. Flow rate 1.0 µl/min. Time 0 is the time of injection.*

4.5.3 Migration of cesium in Cs-OL-SO-conditioned fractures

Cs distribution in the Cs-OL-SO-conditioned columns
Migration of Cs in Cs-OL-SO-conditioned columns was studied with columns that were exposed to ^{134}Cs-spiked Cs-OL-SO for at least six months. The distribution of Cs measured in two clogged mica gneiss columns after six months exposure to $1*10^{-6}$ M Cs and $1*10^{-4}$ M Cs in OL-SO indicate that the concentrations of adsorbed cesium on the rock fracture in the inlet and outlet end are the same (Figure 4-13). The relative Cs sorption as sorption percentage from $1*10^{-6}$ M solution was roughly three times the sorption from $1*10^{-4}$ M solution. The amount of Cs sorbed from $1*10^{-4}$ M Cs-OL-SO is roughly 30 times greater than from $1*10^{-6}$ M solution. Variations in Cs concentration along the flow path are due to mineral distributions in these veined gneiss-type rocks. These results suggest that sorption of Cs is in steady state in the columns taken for further migration experiments of Cs in Cs-OL-SO-exposed columns.

Migration of cesium under constant chemical conditions
Pulse injection experiments were performed with a flow rate 0.9 µl/min on columns G1, KG1, KG3, KG4, GD2, GD3 and GD4. The breakthrough time distribution curves for ^{36}Cl and cesium are collected in Figure 4-14 for the granodiorite and Figure 4-15 for the mica gneiss. It can be seen that the retardation of Cs increases as the concentration decreases, in agreement with higher relative sorption at lower Cs concentrations in earlier batch experiments.

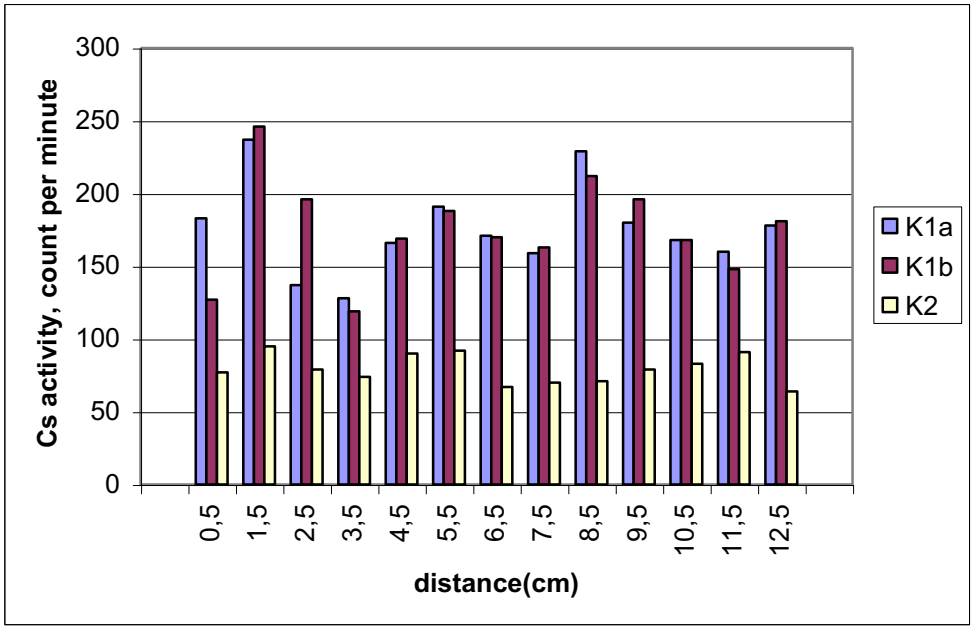

Figure 4-13. *The Cs activity distribution in the clogged columns. The solution Cs concentration was 10^{-6} M in column K1 and 10^{-4} M in column K2. Measurements K1a and K1b were done starting from different ends of the column.*

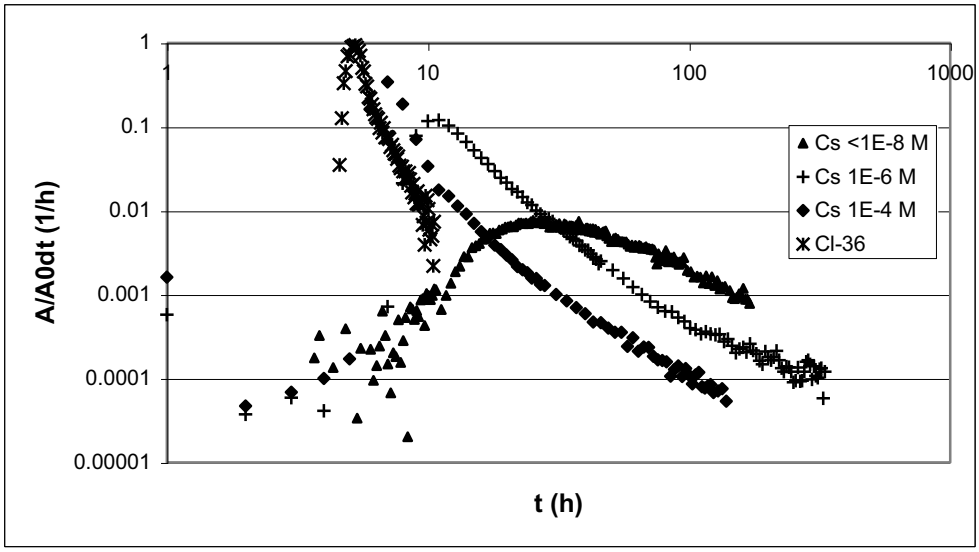

Figure 4-14. *^{132}Cs breakthrough in granodiorite columns, flow rate is 0.9 µl/min.*

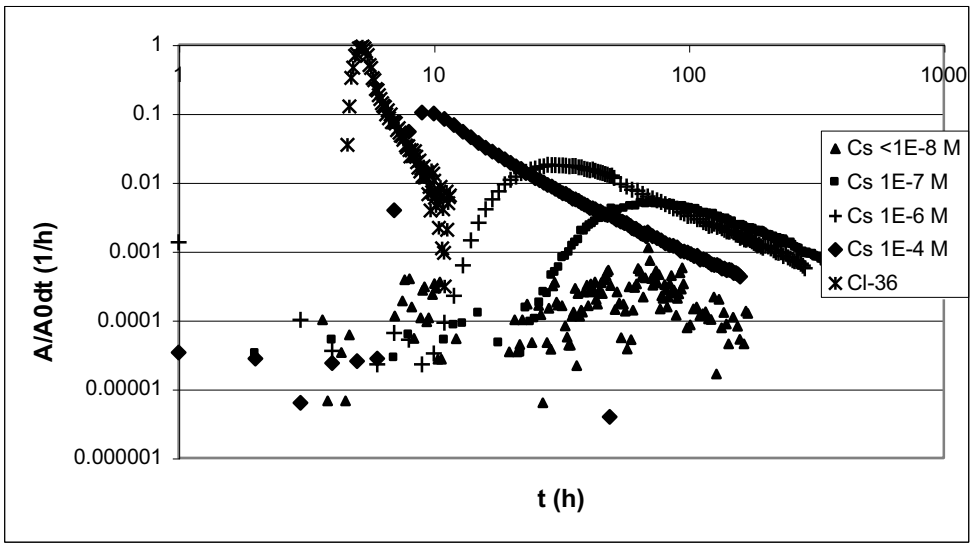

Figure 4-15. *^{132}Cs breakthrough in mica gneiss columns, flow rate is 0.9 µl/min.*

The inventory of the tracer nuclide ^{132}Cs in the effluents was higher than 90% for most of the columns. For column KG4 (10^{-7} M Cs) 64% of injected ^{132}Cs was detected and for the columns with no-carrier-added Cs the inventory of ^{132}Cs in the effluents was 3% in mica gneiss and 47% in granodiorite.

Retardation factors for the maximum in breakthrough relative activities are calculated as $R_f = \frac{V_{Cl}}{V_{Cs}}$ in which V_{Cl} is the velocity of ^{36}Cl in the column and V_{Cs} is the velocity of Cs. As the column length is equal in experiments, this can be reduced

Table 4-8. *Retardation factors (R_f) of Cs in Cs-OL-SO-conditioned fractures*

KG, Cs conc M	R_f	GD, Cs conc M	R_f
Trace	> 34	Trace	32
1E-7	34		
1E-6	9.4	1E-6	2.5
1E-4	2.6	1E-4	1.3

to $R_f = \frac{t_{Cs}}{t_{Cl}}$, in which t_i is the residence time of element i in the column. The retardation factors are in Table 4-8.

The effects of the higher biotite content in mica gneiss can also be seen in these results. The low activity concentrations of trace Cs in mica gneiss compared to $1*10^{-7}$ M Cs effluent suggest very high sorption and/or slow desorption kinetics of trace Cs concentrations.

4.6 Migration of ^{152}Eu in granodiorite fractures

Pulse injection experiments were performed with ^{152}Eu to survey the effect of the presence of Cs in saline ground water on the migration of Eu. Experiments were made on granodiorite column G2 which had been exposed to $1*10^{-6}$ M Cs-OL-SO solution for three years and column GD1 that was conditioned with pure OL-SO. The breakthrough curves are in Figure 4-16.

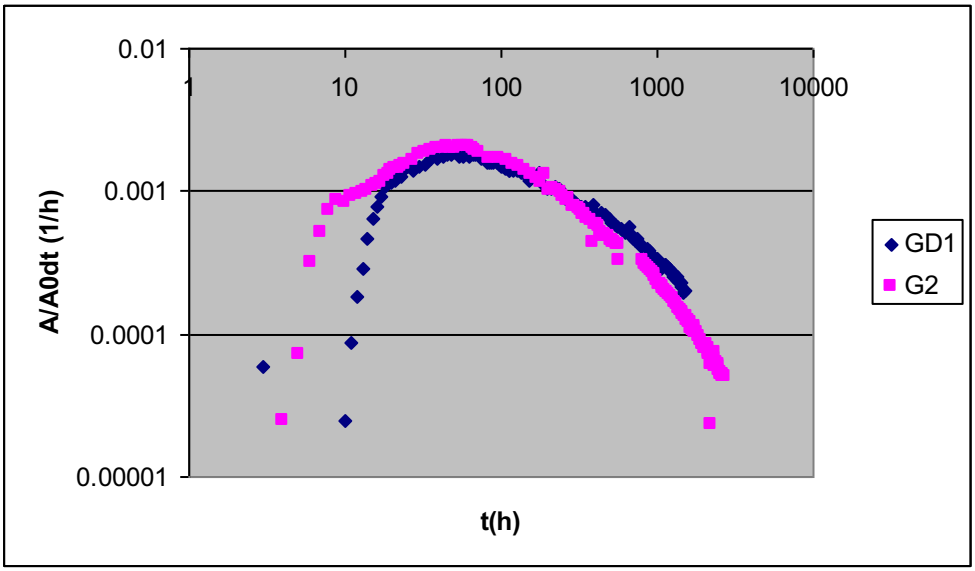

Figure 4-16. *Breakthrough of ^{152}Eu from granodiorite columns G2 (10^{-6}M Cs) and GD1 (no Cs). Flow rate 1 µl/min. A is the fraction activity concentration and A_0 the Eu concentration in the injected solution.*

The collected Eu inventory is higher than 80% for both experiments. The retardation factor for the maximum of the concentration of Eu in the breakthrough in the Cs-OL-SO-conditioned column G2 was 95. Retardation of Eu in the pure OL-SO-conditioned column was 96. The start of the breakthrough in the Cs-conditioned column was earlier. However the effect of Cs on the migration of Eu was marginal. This is in accordance with the estimation that sorption mechanism of cesium and the main OL-SO cations is cation-exchange to the permanently negative sorption sites and sorption of Eu mainly by inner-sphere complexation to variable charge sorption sites in the present salinity and pH conditions. In addition, only the high affinity Cs sorption sites are occupied by Cs and the low affinity sites are occupied by K, Na and Ca.

5 MODELLING

5.1 Model

The sorption and transport-matrix diffusion models in PhreeqC program (Parkhurst and Appelo 1999) were applied. The Windows version was used (Post 2007). In the reactive transport modelling the finite difference approach was applied to take into account the stagnant pore volumes.

5.2 Sorption modelling

The chemical interaction of solutes with the rock surfaces in the transport model was calculated by cation exchange reactions using a three-site model. The interaction was taken to be dominated by sorption onto biotite, the effect of other minerals was assumed to be negligible. Cs sorption isotherms were determined by batch method using Na-, K- and Ca-conditioned biotites (Kyllönen et al. 2008). The isotherms were then modelled using PhreeqC, and the acquired Gaines and Thomas selectivity coefficients in Kyllönen et al. (2008) were used in the modelling. The solute activity coefficients were calculated by the Davis equation.

5.2.1 Batch sorption on rock

The selectivity coefficients and surface site densities for KR9 biotite in Table 4-6 (Kyllönen et al. 2008) were used for modelling the sorption of Cs on crushed mica gneiss in OL-SO solution in Huitti et al. 1998. In the modelling, sorption on the biotite was considered. The modelling results (Figure 5-1) are in good agreement with the experimental values.

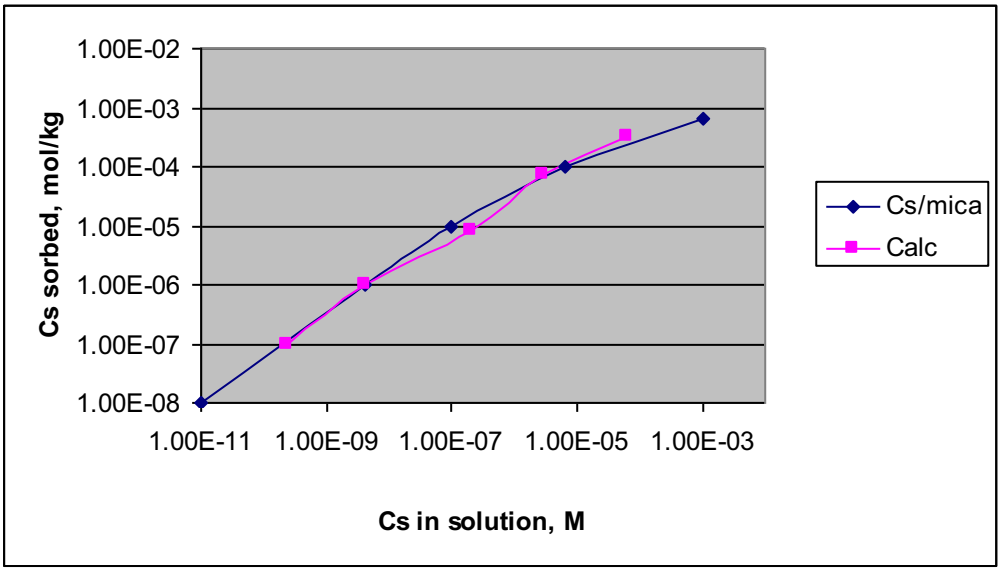

Figure 5-1. *Experimental (Cs/mica) and calculated (Calc) sorption isotherm of Cs for crushed mica gneiss in OL-SO (Huitti et al. 1998, Kyllönen et al. 2008).*

5.3 Transport modelling

5.3.1 Matrix diffusion

The Cs fracture flow migration experiments were first modelled using only the cation exchange model on PhreeqC. The model was first calibrated using breakthrough data of the non-sorbing chloride ($^{36}Cl^-$), and then the Cs breakthrough experiments were modelled by using selectivity coefficients for biotite. Sorption site densities were used as a fitting parameter. With this approach it was possible to predict the residence times of the maximum in the breakthrough Cs pulses, but the model did not produce the tails observed in the breakthrough curves. Thus porosity in the form of stagnant volume was added to the model.

The finite difference approximation was used for the stagnant zone calculations. The fracture length was divided into 40 mobile cells. Rock matrix stagnant volume porosity was abstracted to 10 mm long open pores that were divided into 10 adjacent 1 mm-long cells, one pore connected to each mobile cell. The pores were taken to be rectangular and the width was taken to be the same as the width of the flow channel. The aperture of the pore was equal to give a pore volume two times of the volumetric porosity of the matrix to take into account the porosity of the two fracture walls. The value for the porosity was fixed after fitting of breakthrough of the conservative tracer. In the model the coefficient of effective diffusion (D_e) of all the ions considered in the pores was estimated to have the value of the coefficient in free water, $2*10^{-9}$ m^2/s. Mixing factors were calculated explicitly for the flow rates applying the scheme in the PhreeqC manual.

5.3.2 Transport properties of the fractures

The porosity of the rocks was surveyed by modelling of the breakthrough time distribution on the non-sorbing chloride ion ($^{36}Cl^-$) in the columns. In the model the fracture was divided into 40 mobile cells. A satisfactory fitting of the model to experimental curves was found for a volumetric porosity of 2% for the mica gneiss and the granodiorite (Figure 5-2). The mixing factors corresponding to 2% porosity were used in modelling of transport of Cs in the columns. For that reason, dispersivity in the fracture was set low in the model and more weight was put into fitting of the peak maximum and tailing.

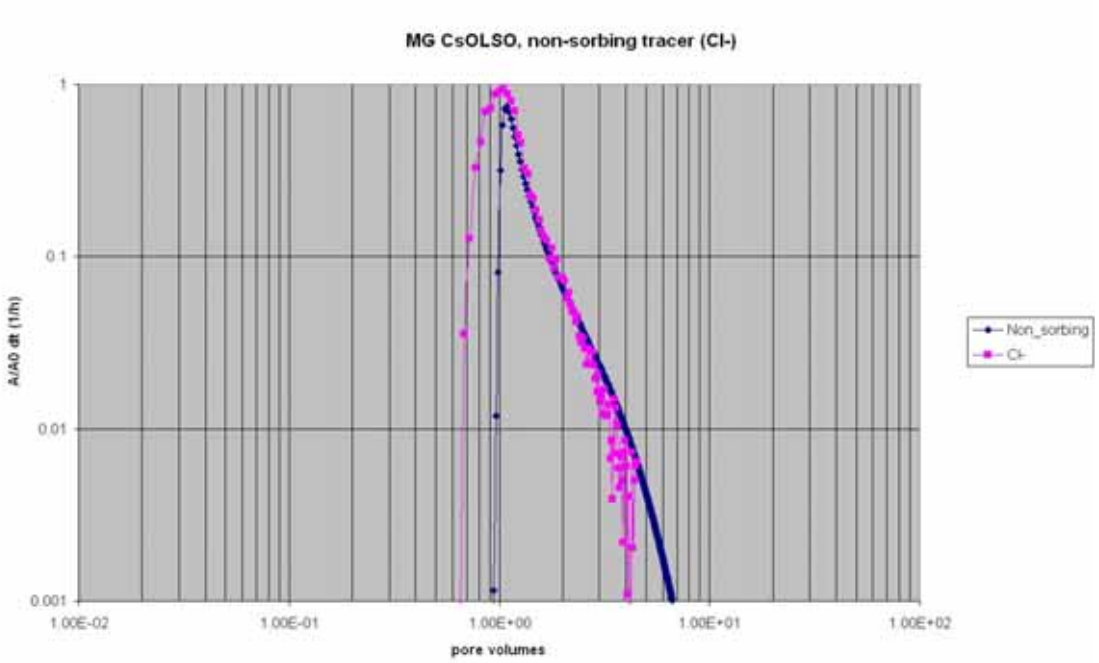

Figure 5-2. *Measured and modelled Cl^- pulse breakthrough on mica gneiss column, flow rate 0.9 µl/min.*

5.3.3 Migration of cesium in Cs-OL-SO-conditioned fractures

Mica gneiss

Three sorption sites were used to model sorption of Cs on biotite for the concentration range $1*10^{-8}$ M to $1*10^{-4}$ M. The selectivity coefficients and activity coefficients were the same as in the modelling on crushed rock. The aim was to have a single set of sorption site concentrations for a rock type.

The sorption model was calibrated using the breakthrough time distributions of pulse-injected ^{132}Cs in mica gneiss fractures. The sorption equilibrium constants for the different sorption sites were the same as for the separated OL biotite but sorption site densities in the columns was estimated to be different from the site densities used in the batch experiments on crushed biotite by Kyllönen et al. (2008). The site concentrations in the flow channel mobile cells and in the stagnant pore cells were used as fitting parameters in modelling. The same ratios of the three sorption sites were used both for the flow channel and the stagnant areas. The aim was to get a single set of sorption site concentrations giving adequate fitting for the different Cs concentrations. The fitted values for the three site concentrations are presented in Table 5-1 and Table 5-2. Site concentrations in the pores were five times those in the mobile cells.

Table 5.1. *Sorption site densities on the fracture surfaces (mobile cells).*

Site	Site density/(mol/L)
X	0.006
Xa	0.0001
Xb	0.0000015

Table 5.2. *Sorption site densities in the matrix (stagnant volume).*

Site	Site density/(mol/L)
X	0.03
Xa	0.0005
Xb	0.0000075

Figures 5-3, 5-4 and 5-5 show satisfactory agreement between the modelled and experimental breakthrough times.

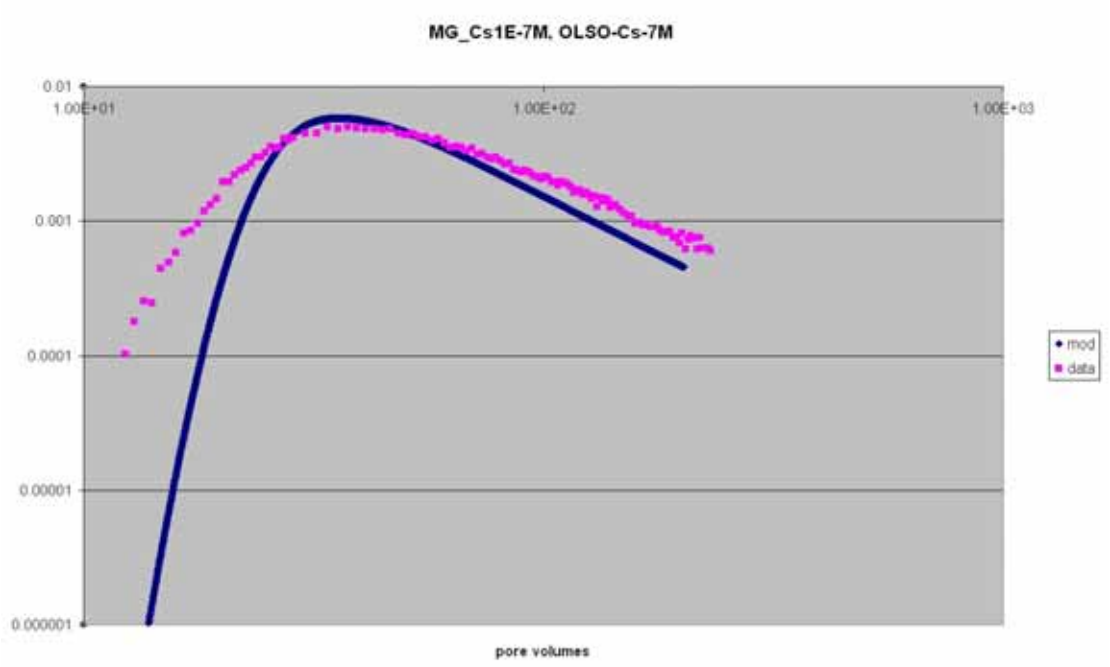

Figure 5-3. *Measured and calculated $1*10^{-7}$ M Cs^{+} pulse breakthrough on mica gneiss column, flow rate 0.9 µl/min. The inventory of the pulse in the experiment was 64%. The concentration scale is for the model and the experimental curve is shifted up for easier comparison of the breakthrough time distributions.*

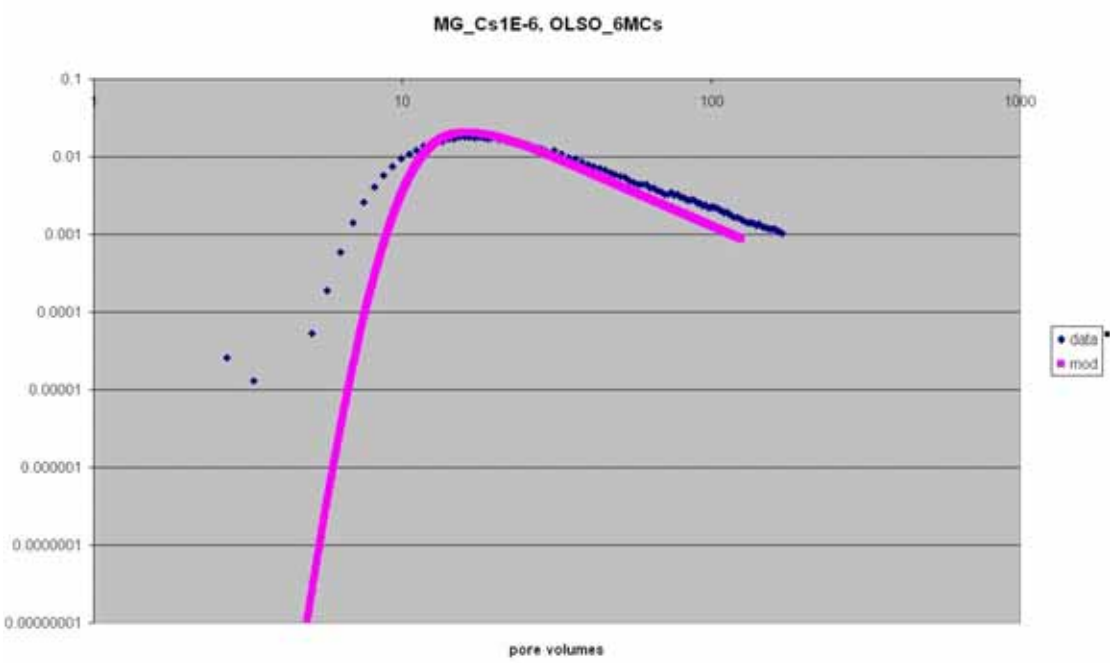

Figure 5-4. *Measured and calculated 1*10^{-6} M Cs^{+} pulse breakthrough on mica gneiss column, flow rate 0.9 µl/min.*

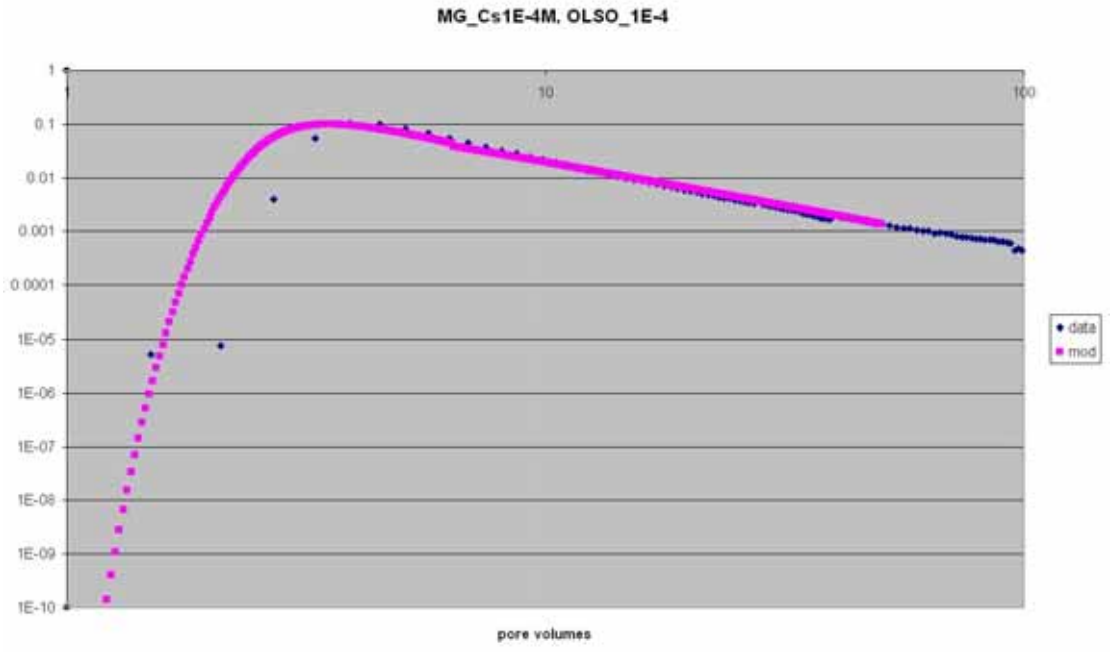

Figure 5-5. *Measured and calculated 1*10^{-4} M Cs^{+} pulse breakthrough on mica gneiss column, flow rate 0.9 µl/min.*

Granodiorite

The model was calibrated using the mica gneiss results, and then tested with results from similar experiments which were performed using granodiorite. The relative proportions of the sorption sites were the same as for mica gneiss. When biotite was taken to be the only sorbing mineral in the rocks the site densities in granodiorite were lower than in mica gneiss. The flow rates in the experiments were equal, 0.9 ul/min, so the mixing factors were the same as for mica gneiss.

It was found that the site densities giving acceptable fittings for Cs migration in a granodiorite fracture were lower than in mica gneiss by a factor of five. This is at the lower end of the ratio of biotite content in mica gneiss to that of the granodiorite rock type in Olkiluoto.

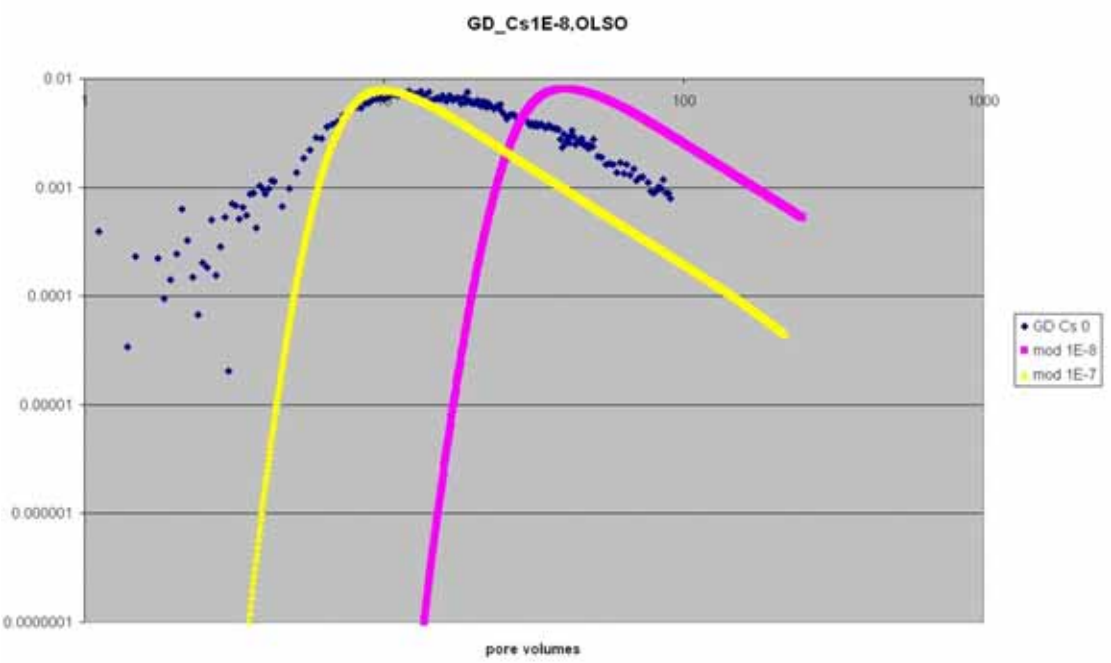

***Figure 5-6**. Measured and calculated 1*10^{-8} M Cs^{+} pulse breakthrough on granodiorite column, flow rate 0.9 µl/min. The model curve 1E-7 was calculated assuming that the Cs concentration was 1*10^{-7} M.*

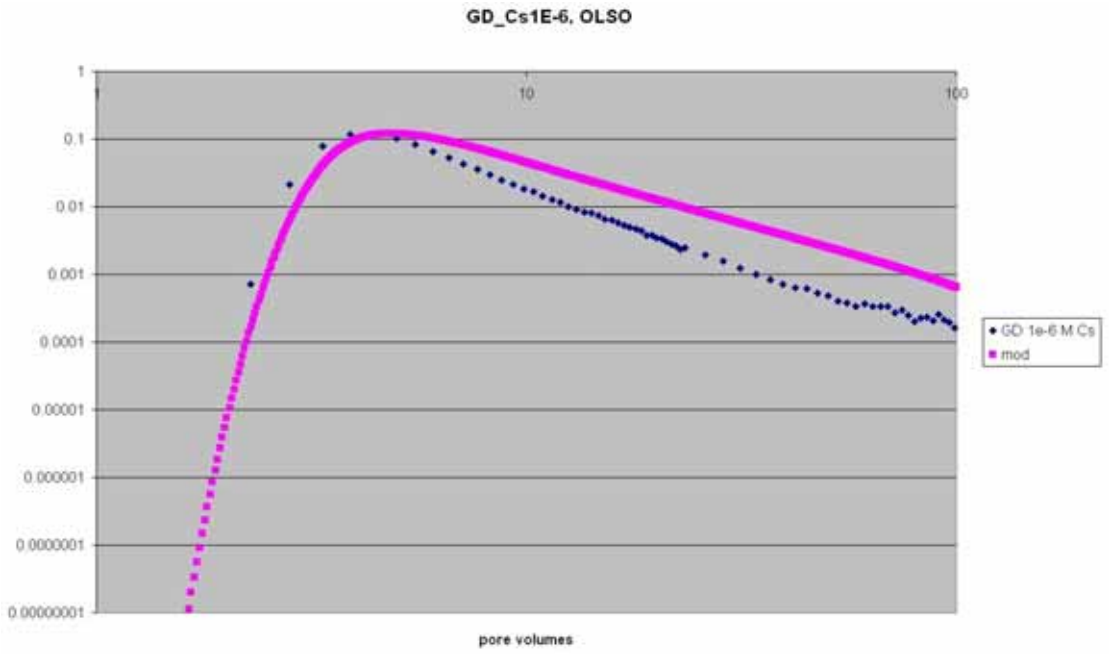

Figure 5-7. *Measured and calculated $1*10^{-6}$ M Cs^{+} pulse breakthrough on granodiorite column, flow rate 0.9 µl/min.*

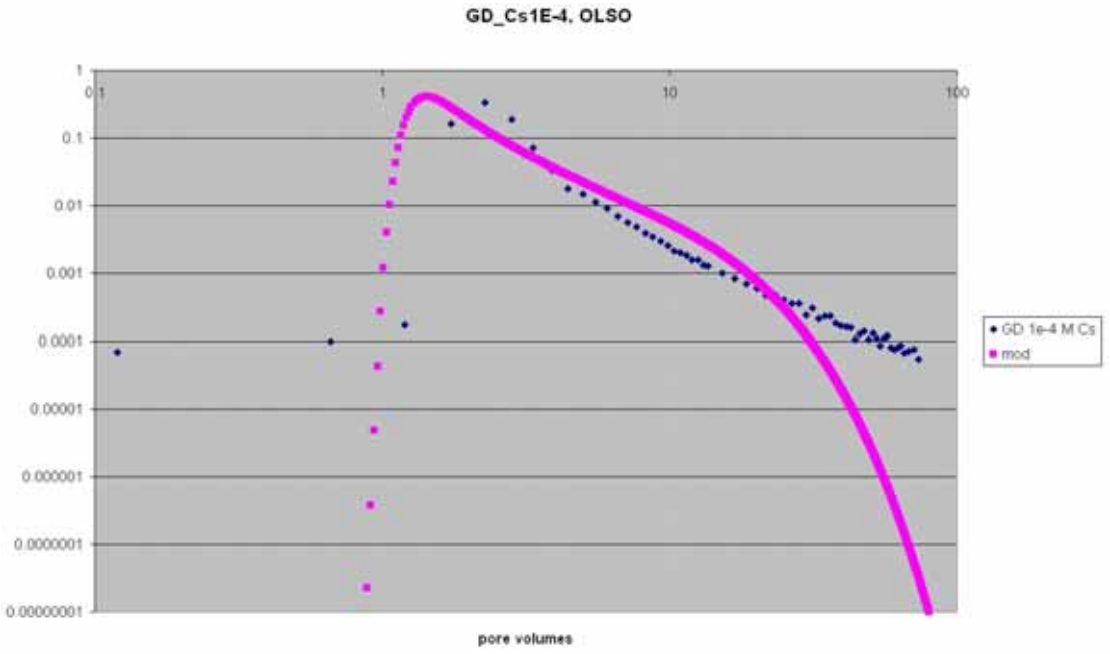

Figure 5-8. *Measured and calculated $1*10^{-4}$ M Cs^{+} pulse breakthrough on granodiorite column, flow rate 0.9 µl/min.*

5.3.4 Breakthrough of cesium in OL-SO-conditioned fractures

Mica gneiss
The model was further tested by modelling the breakthrough front of Cs in OL-SO-conditioned fractures. Breakthrough of Cs in an OL-SO-conditioned mica gneiss fracture after start of continuous injection of $1*10^{-7}$ M Cs-OL-SO solution was modelled using the fracture dimensions, matrix abstraction and sorption site concentrations that were fitted for the Cs-OL-SO-conditioned mica gneiss. The calculated breakthrough time distribution is in fair agreement with the experimental result (Figure 5-9).

The model was also applied to calculation of breakthrough of Cs in OL-SO-conditioned fractures after continuous inflow of $1*10^{-6}$ M Cs-OL-SO at a flow rate of 2.5 µl/min. The values of the mixing factors were recalculated to be in accordance with the flow rate of 2.5 µl/min. The fixed site concentrations for mica gneiss and granodiorite were used. The modelling results slightly overestimate the retardation of Cs in mica gneiss (Figure 5-10) and in the granodiorite fracture especially at larger pore volume values (Figure 5-11).

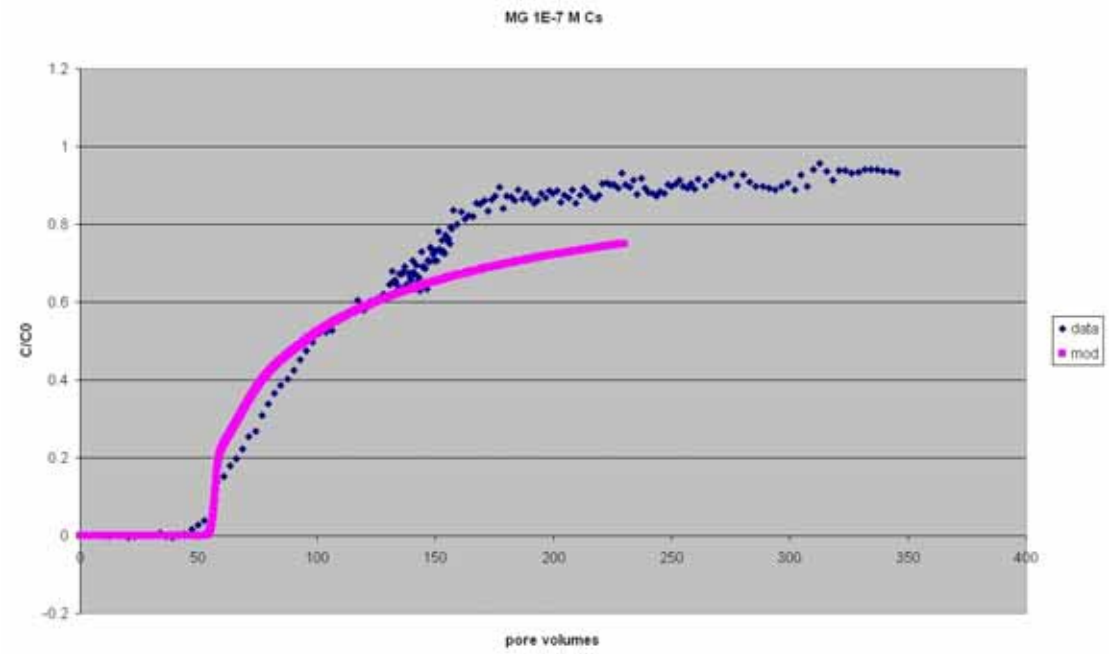

Figure 5-9. *Measured and calculated Cs breakthrough in mica gneiss fracture column, $1*10^{-7}$ M Cs-OL-SO solution; flow rate 1.0 µl/min.*

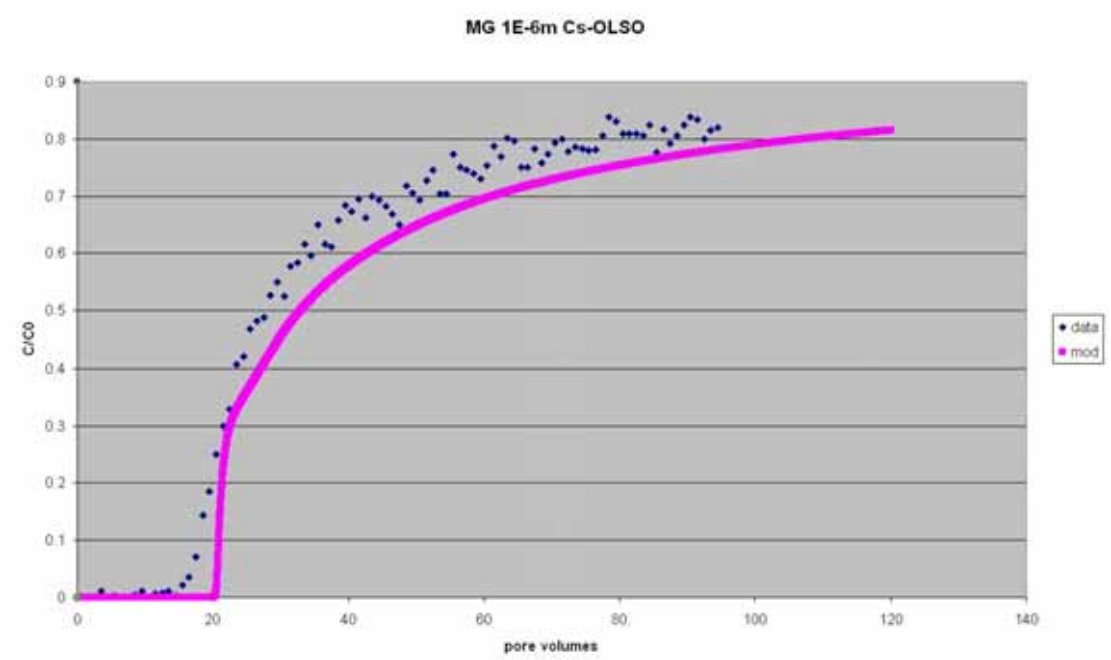

Figure 5-10. *Measured and calculated Cs breakthrough in mica gneiss fracture column, 1*10^{-6} M Cs-OL-SO solution; flow rate 2.5 µl/min.*

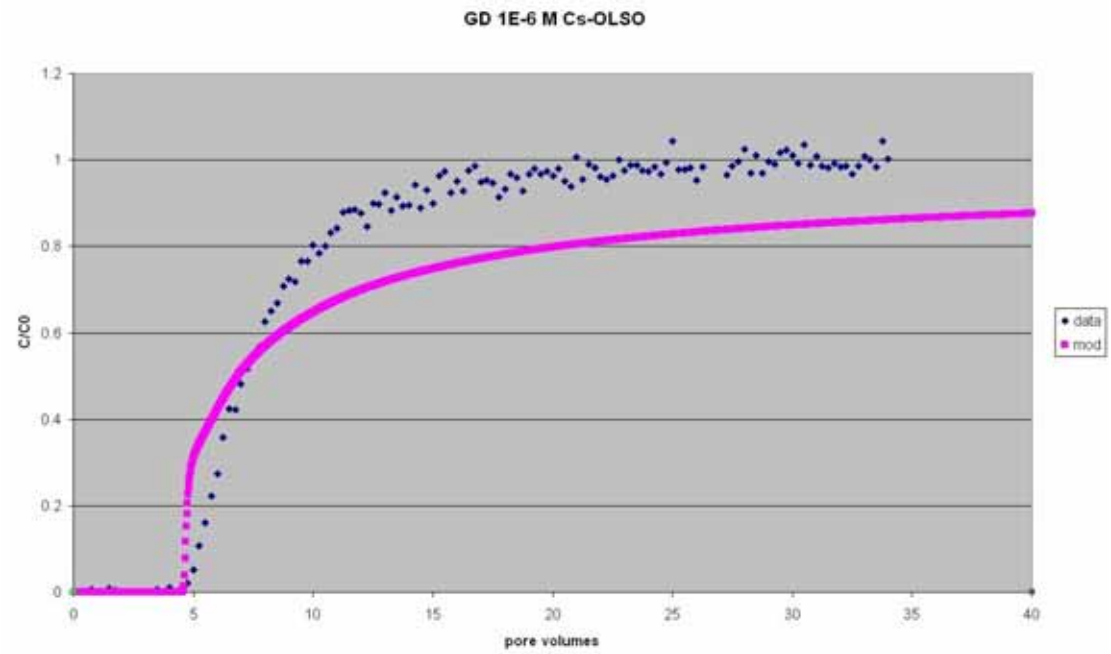

Figure 5-11. *Measured and calculated Cs breakthrough in granodiorite fracture column, 1*10^{-6} M Cs-OL-SO solution; flow rate 2.5 µl/min.*

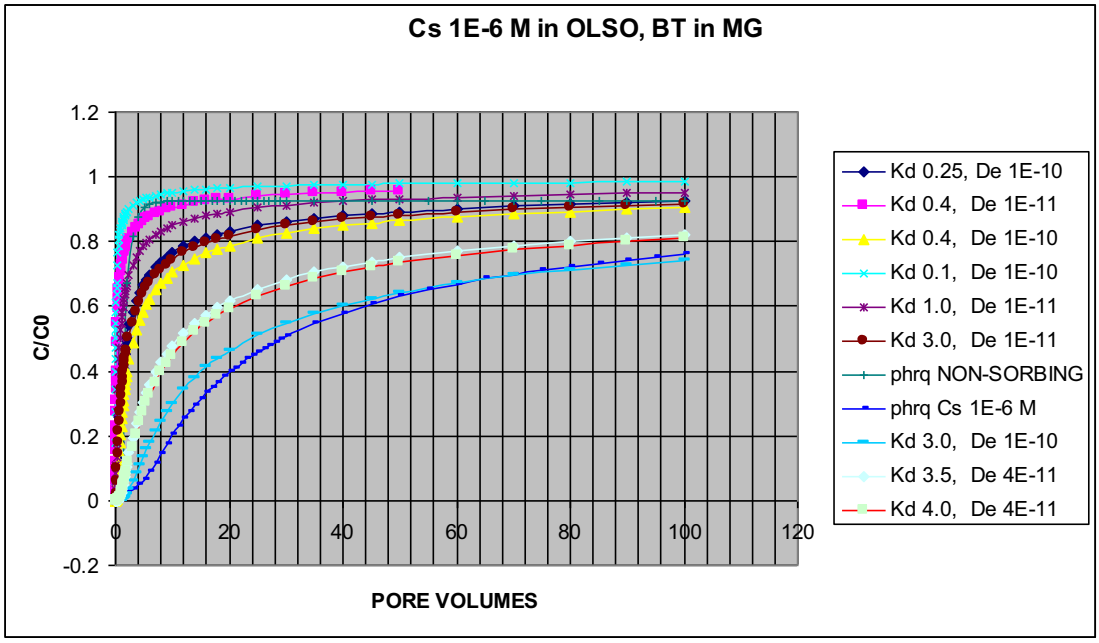

Figure 5-12. *Computed breakthrough of Cs in mica gneiss column after start of continuous introduction of 1*10^{-6} M Cs in OL-SO. Surface sorption on fracture walls is omitted. Comparison of results from analytical model (Vieno 1994) using combinations of K_d (m^3/kg) and D_e (m^2/s) with results from stationary volume sorption only in PhreeqC (phrq Cs).*

The retardation of Cs by the stagnant volume only using PhreeqC was compared with an analytical expression of sorbing solute concentration in a fracture as a function of time and distance from inlet (Vieno 1994). The calculated breakthrough of the sorbing solute is expressed in Figure 5.12 to combinations of mass distribution ratio (K_d, m^3/kg) and coefficient of effective diffusion (D_e, m^2/s). The results for both the analytical expression and PhreeqC indicate breakthrough in less than one fracture pore volume. Including surface sorption (Figure 5-10) the breakthrough was retarded by about 20 pore volumes. At 40 pore volumes and higher the migration of Cs is dominated by matrix properties.

6 SUMMARY

Sorption of cesium on Olkiluoto and Hästholmen rocks in saline and fresh groundwater is strongly non-linear (Huitti et al., 2000, Huitti et al., 1998, Kaukonen et al., 2000). The sorption process of cesium seems to be at least partially irreversible not only at trace cesium concentrations but also at elevated Cs concentrations especially in saline groundwater. Strong sorption non-linearity and partial non-reversibility of cesium on micaceous and clay minerals has been frequently observed. The objective of this project is to study the sorption of cesium on Olkiluoto rocks and their most common mica mineral biotite in more detail.

The rock materials used in the experiments were mica gneiss and granodiorite from Olkiluoto. Biotite for this study was separated from crushed rocks. The experimental program included batch sorption experiments with rock samples to determine the sorption isotherms and mass balances in cesiun sorption and dynamic fracture column migration experiments.

Determination of the mass balance of exchangeable cations in the sorption was studied by analysis of the solutions. The accuracy of the chemical analysis was sufficient only in the Allard water to see the changes owing to sorption of cesium. Experiments with rocks that were not preconditioned with Allard solution indicated that mineral solution interactions also other than sorption of cesium affected the solution compositions and that the changes were different for the different rock types. Experiments with Allard conditioned rocks showed sorption mass balances that indicate sorption by cation exchange as expected. The mass balances showed that in Olkiluoto rocks the sorption of cesium takes place mainly by exchange for bound sodium and calcium. The exchange for bound potassium was a minor reaction.

The exchangeable cations in OLKR2 and OLKR9 biotites and in a pegmatitic biotite of another origin were determined by exchange of the bound cations for alkaline and earth alkaline cations and ammonium ion. These results also showed that in the OL biotites the main exchangeable cations are calcium and sodium. In the pegmatitic biotite the main exchangeable cation was potassium. These results indicated that the OL biotites behave quite differently from the pegmatitic biotites. The microanalyses of the OLKR2 and OLKR9 biotites are typical to biotites in Olkiluoto in general. The sum of equivalents of the exchanged cations was calculated to determine the cation exchange capacity (CEC) of the biotites. CEC of OL biotites was also determined by ammonium acetate and silver thiourea (AgTU) methods. The value adopted for further use is 18 μeq/g .

The OLKR9 biotite was conditioned to Na^+-, K^+- and Ca^{2+}-forms for determination of equilibrium constants of binary cation exchange reaction with cesium. The experiments were performed and the results were interpreted by using a three-site model. Gaines and Thomas selectivity coefficients were derived for exchange of K^+, Cs^+ and Ca^{2+} for bound Na^+. The values were used in PhreeqC for modelling the batch cesium sorption isotherms experiments (Huitti et al.1998) for mica gneiss in OL-SO solution by assuming that the sorption was determined by the biotite in the solid. The calculated

values are in good accord with the experimental results for the whole cesium concentration range.

Experiments were performed to determine the dependence of breakthrough time of cesium concentration in OL-SO-conditioned mica gneiss and granodiorite fracture columns. After attainment of also cesium equilibrium of the fracture surface the migration of cesium was determined by surveying breakthrough time distribution of pulse-injected ^{132}Cs tracer.

The column experiments were modelled using PhreeqC. The flow properties of the columns were used for determination of the matrix stagnant volume. The breakthrough time distribution of the non-sorbing chloride ion was modelled using a 40 mobile cell path and applying the finite difference approach in PhreeqC for the stagnant volume. The stagnant volume was abstracted, omitting constrictivity and tortuosity, by an open pore connected to each mobile cell. A pore was constructed of 10 adjacent 1 mm-long cells. By varying the volume (porosity) the best fit for the breakthrough pulse tailing was found for a stagnant volume of 2%. This value was used for modelling of migration of cesium.

The site concentrations of the three sorption sites of biotite in the rock were used as fitting parameters in modelling of migration of cesium in the Cs-OL-SO-conditioned fractures. The ratios of the sites were the same in the mobile cells and in the stagnant volume but the site concentrations in the stagnant volume were further used as fitting parameters. The experimental results for the mica gneiss were used for calibration of the model. By only changing the cesium concentration the model produced the experimental breakthrough curves adequately. The model was applied to calculation of migration of cesium in granodiorite fractures. Since the biotite concentration of granodiorite is lower than in mica gneiss the site densities in the mica gneiss model were reduced by a constant ratio. An adequate fit was found when the site concentrations were a fifth of those in mica gneiss. This is at the lower limit of ratio of biotite contents in these rock types.

The breakthrough fronts of cesium in the OL-SO-conditioned mica gneiss and granodiorite fractures were modelled by using the sorption parameters obtained for the rock types. The mixing factors for the finite difference matrix calculation were explicitly calculated to the different flow rates. The model results reproduce the breakthrough times but slightly overestimate breakthrough concentrations after breakthrough.

Breakthrough of cesium in mica gneiss for $1*10^{-6}$ M Cs in OL-SO was calculated by PhreeqC omitting the surface sorption. The results indicate that in the long run matrix diffusion is dominant in the breakthrough, but the time of start of breakthrough is determined by surface sorption. An analytical approach for the same situation with a K_d for sorption and D_e for matrix diffusion was used for comparison. High sorption and large D_e value (in accordance with 2% porosity) was needed to reproduce the long-term breakthrough of cesium in the OL-SO-conditioned fracture.

REFERENCES

Blum A.E., Stillings L.L. 1995. Feldspar dissolution kinetics. Rev.Mineral. 1995, 31, 291-351. ISSN 0275-0279.

Chapman H.D. 1965. Cation-exchange capacity. In: C. A. Black (ed.) Methods of soil analysis - Chemical and microbiological properties. Agronomy 9: 891-901.

Chhabra R., Pleysier J., Cremers A. 1975. The measurement of the cation exchange capacity and exchangeable cations in soils:a new method. Proc. Int. Clay Conf. 1975, Applied Publishing Ltd, Wimele, Illinois. USA

Dove P.M. 1995. Kinetic and thermodynamic controls on silica reactivity in weathering environments Rev.Mineral. 31, 235-290. ISSN 0275-0279

Gehör S., Kärki A., Määttä T., Suoperä S:, Taikina-aho O. 1996. Eurajoki, Olkiluoto: Petrology and low temperature fracture minerals in drill core samples. Posiva Working Report PATU-96-42 (in Finnish)

Hakanen M., Huitti T. 2001. Reversibility of Radionucide Sorption- a literature research. Posiva Working Report TR 2001-21. (in Finnish)

Huitti T., Hakanen M. and Lindberg A. 1998. Sorption of cesium on Olkiluoto mica gneiss, granodiorite and granite. POSIVA 98-11. ISBN 951-652-049-9.

Huitti T., Hakanen M., Lindberg A., 2000. Sorption and desorption of cesium on rapakivi granite and its minerals. POSIVA 2000-03. ISSN 1239-3096

Huitti et al, 2001. Cesiumin sorptio Olkiluodon kiillegneissiin ja granodioriittiin jatkuvassa Cs-altistuksessa -kokeiden käynnistäminen ja tulokset vuonna 2000 tehdyistä kokeista. Posiva TR 2001-22

Hölttä P., Hakanen M., Hautojärvi A., Timonen J., and Väätäinen K. 1996. The effects of matrix diffusion on radionuclide migration in rock column experiments. J.Contam.Hydrol. 21, 165-173.

Kaukonen V., Hakanen M. and Lindberg A. 2000. Sorption and desorption of cesium on intact Olkiluoto rock samples. POSIVA Working Report 2000-13.

Kyllönen J. et al. 2008. to be published.

Lindberg A. 2001. The stability of biotite in the conditions of final disposal at Olkiluoto- a literature study. Posiva Working Report 2001-12.

McEwen T. and Äikäs T. 2000. The site selection process for a spent fuel repository in Finland - Summary report. POSIVA 2000-15. ISSN 1239-3096

Parkhurst D., Appelo C.A.J. 1999. Users guide to PhreeqC (Version 2). A Computer Programm for Speciation, Batch-Reaction, One-Dimensional Transport, and Inverse Geochemical Calculations. Water Resources Investigations Report 99-4259. US. Geological Survey Denver, Colorado.

Post V. 2007. www.geo.vu.nl/users/posv/phreeqc/download.HTML

Steefel C.I., Carroll S., Zhao P., Roberts S. 2003 Cesium migration in Hanford sediment: A multisite cation exchange model based on laboratory transport experiments. J.Contam.Hydrol. 67(2003), 219-246.

Vieno T., Nordman H., 1996. Interim report on safety assessment of spent fuel disposal. TILA 96. POSIVA 96-17. ISSN 1239-3096

Vieno T., 1994. Safety Analysis of Disposal of Spent Nuclear Fuel, VTT Publications 177, Technical Research Centre of Finland, Espoo.

Vuorinen U., Ollila K., Snellman M. 1997. Olkiluodon pohjavesikemia -suolainen ja murtovesi- suolaisen referenssiveden resepti. POSIVA Työraportti-97-25.

Vuorinen U., Snellman M. 1998. Finnish reference waters for solubility, sorption and diffusion studies. POSIVA Working Report 98-61.

Zachara J., M., McKinley J., P., Serne R., J., Smith S., C., Gassman P., L. 2000. Mineral Structure Controls on Cs Adsorption in Hanford Sediments. Environmental Dynamics Simulation 1999 Annual Report. William R.Wiley Environmental Molecular Sciences Laboratory, Richland, WA.

APPENDIX A

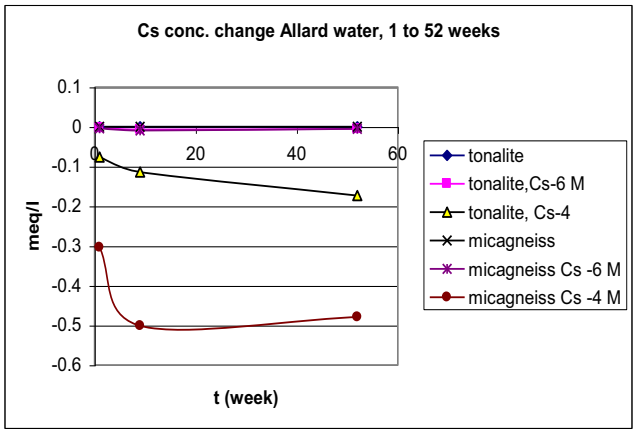

Figure A1. *Cesium concentration changes (meq/l) in Allard water from different Cs concentrations ($5*10^{-4}$ M and $5*10^{-6}$ M).*

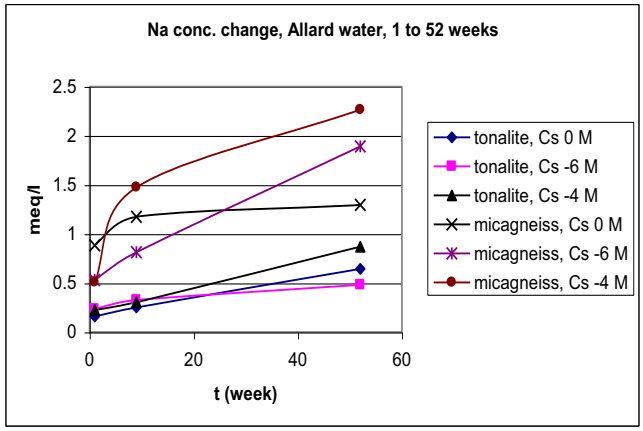

Figure A2. *Sodium concentration changes (meq/l) in Allard water from different Cs concentrations ($5*10^{-4}$ M and $5*10^{-6}$ M).*

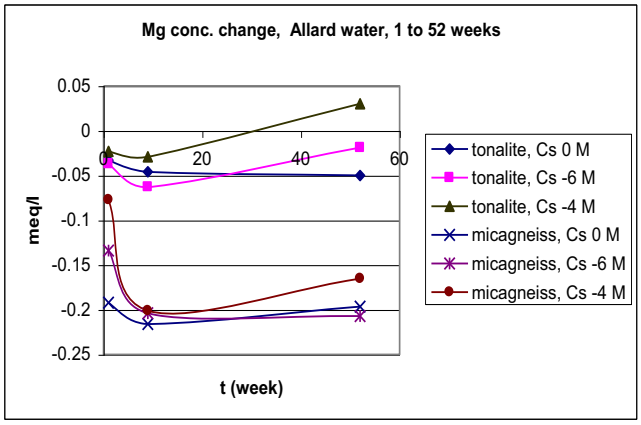

Figure A3. *Magnesium concentration changes (meq/l) in Allard water from different Cs concentrations ($5*10^{-4}$ M and $5*10^{-6}$ M).*

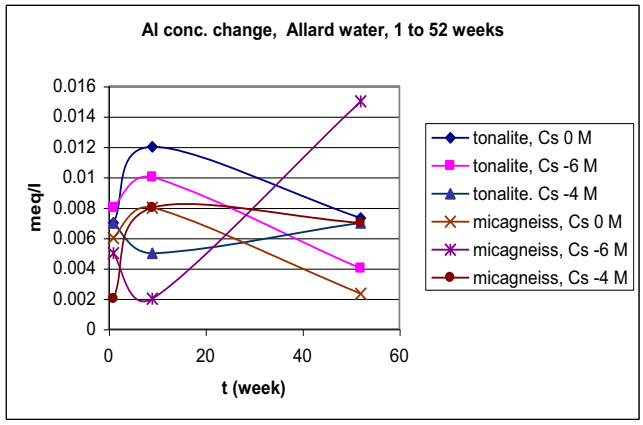

Figure A4. *Aluminium concentration changes (meq/l) in Allard water from different Cs concentrations ($5*10^{-4}$ M and $5*10^{-6}$ M).*

APPENDIX A CONT.

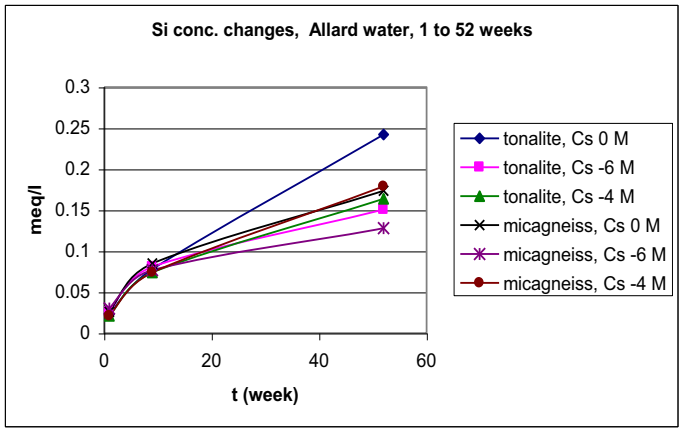

Figure A5. *Silicon concentration changes (meq/l) in Allard water from different Cs concentrations ($5*10^{-4}$M and $5*10^{-6}$M).*

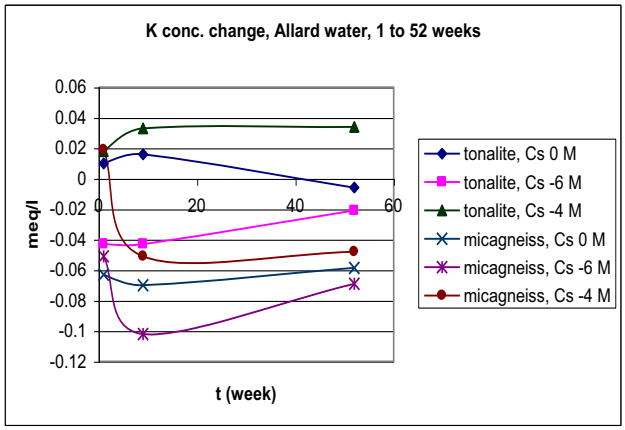

Figure A6. *Potassium concentration changes (meq/l) in Allard water from different Cs concentrations ($5*10^{-4}$M and $5*10^{-6}$M).*

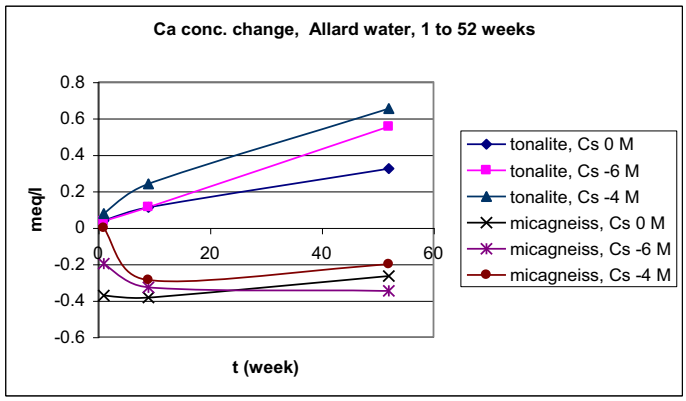

Figure A7. *Calcium concentration changes (meq/l) in Allard water from different Cs concentrations ($5*10^{-4}$M and $5*10^{-6}$M).*

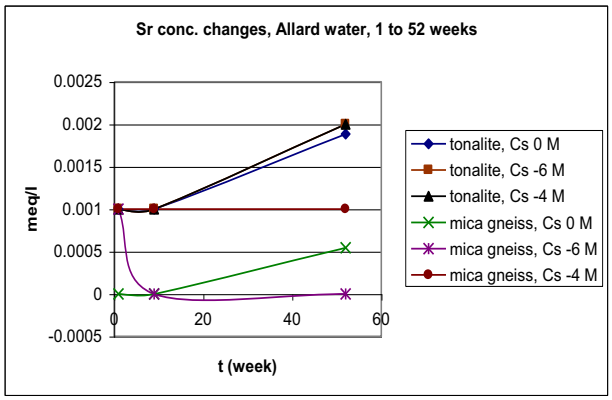

Figure A8. *Strontium concentration changes (meq/l) in Allard water from different Cs concentrations ($5*10^{-4}$M and $5*10^{-6}$M).*

APPENDIX B

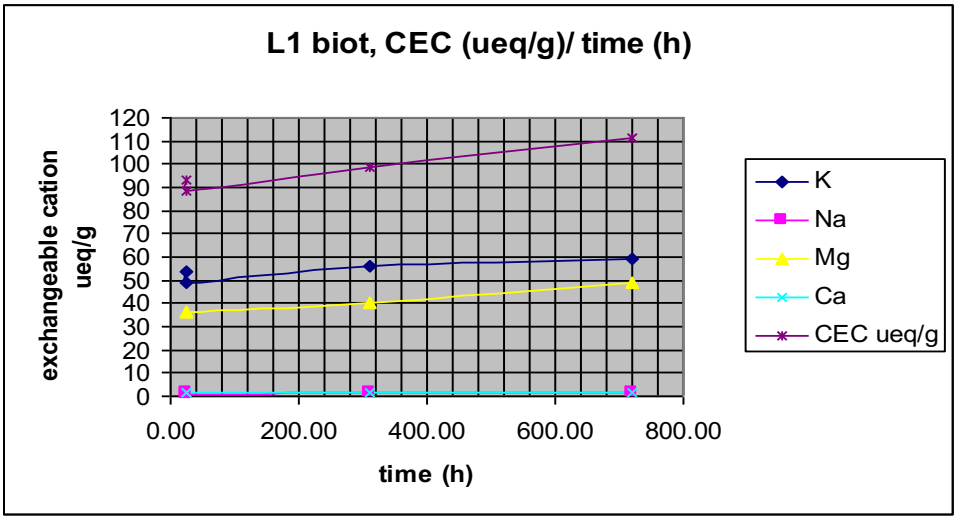

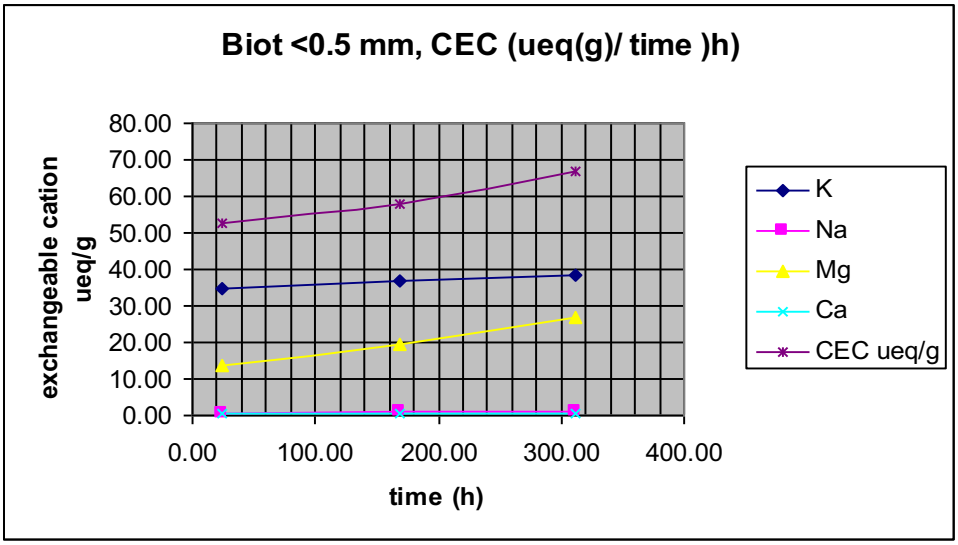

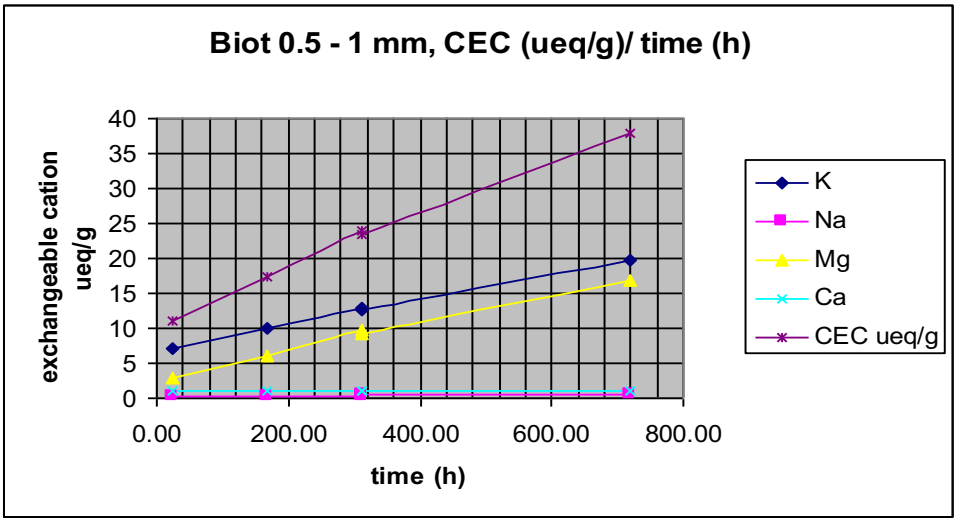

Figure B1. *Time dependence of charge equivalent concentrations of K, Na, Mg and Ca in 1M NH_4Ac solution for different size fractions of L1 biotite. L1 < 0.1 mm, Biot < 0.5 mm, Biot 0.5 - 1 mm.*